

Server and data center 3 kW 50 V PSU

EVAL_3KW_50V_PSU



About this document

Authors

Manuel Escudero, Matteo-Alessandro Kutschak, David Meneses

Scope and purpose

This document introduces a complete Infineon's system solution for a 3 kW power supply unit (PSU) targeting the newly released OCP rectifier V3 specifications for servers and data centers.

The PSU comprises a front-end AC-DC bridgeless totem pole converter followed by a back-end DC-DC isolated half-bridge LLC converter. The front-end totem pole converter provides power factor correction (PFC) and total harmonic distortion (THD). The LLC converter provides safety isolation and a tightly regulated output voltage.

The measured peak efficiency of the complete PSU at 230 V_{AC} is 97.5 percent, not including the internal fan, and 97.4 percent, including the internal fan. The overall outer dimensions of the PSU are 73.5 mm x 520 mm x 40 mm, which yields a power density in the range of 32 W/inch³ (1.95 W/cm³).

This document describes the converter hardware, a summary of the experimental results and several design recommendations for the complete Infineon solution, also including an innovative in-house planar magnetic construction.

The main Infineon components used in the EVAL_3KW_50V_PSU are:

- CoolSiC™ 650 V 48 mΩ ([IMZA65R048M1H](#)) in the totem pole PFC half-bridge
- 600 V CoolMOS™ 17 mΩ ([IPW60R017C7](#)) in the totem pole PFC synchronous rectifiers (SRs)
- 600 V CoolMOS™ CFD7 24 mΩ ([IPW60R024CFD7](#)) in the LLC primary-side half-bridge
- OptiMOS™ 5 80 V 3.7 mΩ ([BSC037N08NS5](#)) in the LV bridge
- EiceDRIVER™ [1EDB8275F](#) and [1EDB9275F](#), single-channel drivers for CoolMOS™, CoolSiC™ and CoolGaN™
- EiceDRIVER™ [2EDF7275F](#) dual-channel driver for CoolMOS™, CoolSiC™ and OptiMOS™
- XMC1404 microcontroller for the totem pole PFC control implementation ([XMC1404-LQFP-64](#))
- XMC4200 microcontroller for the LLC control implementation ([XMC4200-F64k256AB](#))

Reference board/kit

Product(s) embedded on a PCB, with focus on specific applications and defined use cases that can include software. PCB and auxiliary circuits are optimized for the requirements of the target application.

Note: Boards do not necessarily meet safety, EMI and quality standards (for example UL, CE) requirements.

Table of contents

Table of contents

About this document..... 1

Table of contents..... 2

Safety information – your safety is our goal..... 3

Important notice 3

Operating instructions 3

Safety precautions..... 4

1 The board at a glance..... 5

1.1 Main features 6

1.2 Block diagram..... 7

2 System and functional description 9

2.1 Bridgeless totem pole PFC..... 10

2.1.1 Totem pole PFC magnetics..... 11

2.2 Half-bridge LLC..... 11

2.2.1 Half-bridge LLC magnetics..... 12

3 Experimental results 14

3.1 Totem pole PFC 14

3.1.1 Boost diode operation 14

3.1.2 Boost switch operation..... 15

3.1.3 SRs polarity detection..... 17

3.1.4 Soft-start..... 18

3.2 Half-bridge LLC..... 19

3.2.1 ZVS switching 20

3.2.2 Soft-start..... 21

3.2.3 Output voltage ripple..... 22

3.2.4 Resonant capacitor voltage 23

3.3 Power supply unit..... 24

3.3.1 Hold-up time 25

3.3.2 Temperature..... 26

3.3.3 Efficiency 27

3.3.4 Power factor and THD 27

3.3.5 EMI 28

4 Design tips..... 30

4.1 Driving 4-pin CoolSiC™ 30

4.2 Driving 3-pin CoolMOS™ 30

4.3 Driving the ORing OptiMOS™ 31

4.4 Driving the SR OptiMOS™ 32

4.5 Generating the multiple auxiliary driving voltages..... 32

5 Schematics..... 34

5.1 Main board..... 34

5.2 Control card..... 35

5.3 Bill of materials..... 36

6 References and appendices 41

6.1 Abbreviations and definitions..... 41

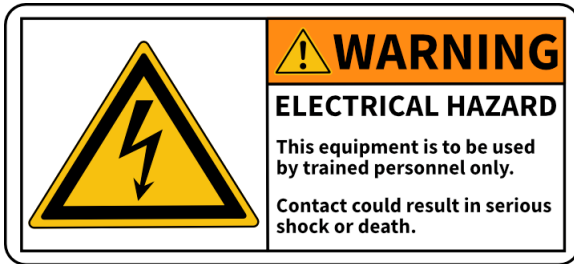
6.2 References 41

Revision history..... 42

Safety information – your safety is our goal

Safety information – your safety is our goal

Please read this document carefully before starting up the device.



Important notice

Evaluation boards, demonstration boards, reference boards and kits are electronic devices typically provided as an open-frame and unenclosed printed circuit board (PCB) assembly. Each board is functionally qualified by electrical engineers and strictly intended for use in development laboratory environments. Any other use and/or application is strictly prohibited. Our boards and kits are solely for qualified and professional users who have training, expertise and knowledge of electrical safety risks in the development and application of high voltage electrical circuits.

Please note that evaluation boards, demonstration boards, reference boards and kits are provided “as is” (i.e. without warranty of any kind). Infineon is not responsible for any damage resulting from the use of its evaluation boards, demonstration boards, reference boards or kits.

To make our boards as versatile as possible, and to give you (the user) opportunity for the greatest degree of customization, the virtual design data may contain different component values than those specified in the bill of materials (BOM). In this specific case, the BOM data has been used for production.

Before operating the board (i.e. applying a power source), please read the application note/user guide carefully and follow the safety instructions. Please check the board for any physical damage which may have occurred during transport. If you find damaged components or defects on the board, do not connect it to a power source. Contact your supplier for further support. If no damage or defects are found, start the board up as described in the user guide or test report. If you observe unusual operating behavior during the evaluation process, immediately shut off the power supply to the board and consult your supplier for support.

Operating instructions

Do not touch the device during operation, and keep a safe distance.

Do not touch the device after disconnecting the power supply, as several components may still store electrical voltage and can discharge through physical contact. Several parts, like heatsinks and transformers, may still be very hot. Allow the components to cool before touching or servicing.







All work such as construction, verification, commissioning, operation, measurements, adaptations and other work on the device (applicable national accident prevention rules must be observed) must be done by trained personnel. The electrical installation must be completed in accordance with the appropriate safety requirements.

Safety precautions

Safety precautions

Note: Please note the following warnings regarding the hazards associated with development systems.

Table 1 Safety precautions

	<p>Warning: The evaluation or reference board contains DC bus capacitors, which take time to discharge after removal of the main supply. Before working on the converter system, wait five minutes for capacitors to discharge to safe voltage levels. Failure to do so may result in personal injury or death. Darkened display LEDs are not an indication that capacitors have discharged to safe voltage levels.</p>
	<p>Warning: The evaluation or reference board is connected to the AC input during testing. Hence, high-voltage differential probes must be used when measuring voltage waveforms by oscilloscope. Failure to do so may result in personal injury or death. Darkened display LEDs are not an indication that capacitors have discharged to safe voltage levels.</p>
	<p>Warning: Remove or disconnect power from the converter before you disconnect or reconnect wires, or perform maintenance work. Wait five minutes after removing power to discharge the bus capacitors. Do not attempt to service the drive until the bus capacitors have discharged to zero. Failure to do so may result in personal injury or death.</p>
	<p>Caution: The heatsink and device surfaces of the evaluation or reference board may become hot during testing. Hence, necessary precautions are required while handling the board. Failure to comply may cause injury.</p>
	<p>Caution: Only personnel familiar with the converter, power electronics and associated equipment should plan, install, commission, and subsequently service the system. Failure to comply may result in personal injury and/or equipment damage.</p>
	<p>Caution: The evaluation or reference board contains parts and assemblies sensitive to electrostatic discharge (ESD). Electrostatic control precautions are required when installing, testing, servicing or repairing the assembly. Component damage may result if ESD control procedures are not followed. If you are not familiar with electrostatic control procedures, refer to the applicable ESD protection handbooks and guidelines.</p>
	<p>Caution: A converter that is incorrectly applied or installed can lead to component damage or reduction in product lifetime. Wiring or application errors such as undersizing the cabling, supplying an incorrect or inadequate AC supply, or excessive ambient temperatures may result in system malfunction.</p>

1 The board at a glance

Due to the increasing power demand in server and data center applications the requirements of power density and efficiency for the Power Supply Units raise continuously. This is due to the operational cost of the infrastructure: on the one hand the cost of the electricity and on the other hand the cost of the space and maintenance of the installations.

Moreover, the high reliability demand in the server and data center applications has a severe impact in the hold-up requirements, which can be as large as 20 ms delivering full power.

This tendencies in power density, efficiency and reliability requirements can be observed in the newly released OCP rectifier V3 specifications for server and datacenter PSU [1]-[2]. The main changes in relation to the previous PSU specifications (Open Rack V1 and V2) are the higher requirements in terms of efficiency (97.5 percent peak) and power density (1.96 W/cm³ or 32.15 W/inch³), together with the large hold-up time (20 ms at full power). Moreover, the maximum outer dimensions of the PSU are 520 mm x 73.5 mm x 40 mm. However, the output voltage has been increased to 50 V_{dc}, although still in a narrow range, which should help with achieving the challenging target specifications.

Infineon has designed and built an evaluation board targeting the OCP rectifier V3 specifications. **Figure 1** shows a photograph of the PSU outside of its chassis. The PSU comprises two stages: a front-end bridgeless totem pole PFC, which provides PFC and THD, followed by an isolated half-bridge series-parallel resonant converter (LLC), which provides a tightly regulated output.

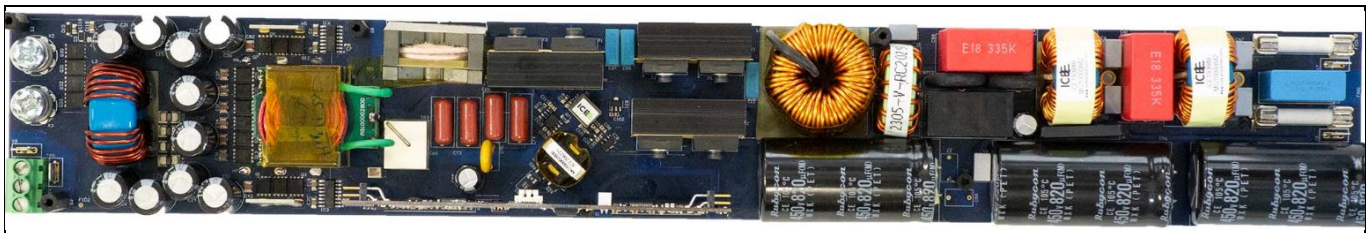


Figure 1 Photo of the EVAL_3KW_50V_PSU – outside of its chassis

Most noticeably, the EVAL_3KW_50V_PSU converter has been designed with Infineon power semiconductors as well as Infineon drivers and controllers. The main Infineon components used in the EVAL_3KW_50V_PSU are:

- CoolSiC™ 650 V 48 mΩ (**IMZA65R048M1H**) in the totem pole PFC half-bridge
- 600 V CoolMOS™ 17 mΩ (**IPW60R017C7**) in the totem pole PFC SRs
- 600 V CoolMOS™ CFD7 24 mΩ (**IPW60R024CFD7**) in the LLC primary-side half-bridge
- OptiMOS™ 5 80 V 3.7 mΩ in SuperSO8 package (**BSC037N08NS5**) in the LV bridge
- EiceDRIVER™ **1EDB8275F** single-channel driver for CoolMOS™, CoolSiC™ and CoolGaN™
- EiceDRIVER™ **1EDB9275F** single-channel driver for CoolMOS™, CoolSiC™ and CoolGaN™
- EiceDRIVER™ **2EDF7275F** dual-channel driver for CoolMOS™, CoolSiC™ and OptiMOS™
- **ICE2QR2280G** QR flyback controller with built-in 800 V CoolMOS™ 2.26 Ω for the auxiliary supply
- XMC1404 microcontroller for the totem pole PFC control implementation (**XMC1404-LQFP-64**)
- XMC4200 microcontroller for the LLC control implementation (**XMC4200-F64k256AB**)
- **IFX91041EJ V33** DC-DC step-down voltage regulator
- Medium-power Schottky diode **BAT165**

The board at a glance

The rest of this document describes the system and hardware of the EVAL_3KW_50V_PSU, as well as the design specification requirements and a summary of the main test results. For further information on Infineon semiconductors see the Infineon website, as well as the Infineon evaluation board search tool, and the websites for the different implemented components.

1.1 Main features

Table 2 and **Figure 2** are a summary of the main specifications and requirements of the OCP V3 rectifier. A more detailed and complete specification can be found in [2].

Table 2 Summary of the requirements and specifications for the OCP rectifier V3 PSU [2]

Requirements	Conditions	Specification
Input voltage V_{in}	180 V _{AC} to 275 V _{AC}	230 V _{AC} nominal
Output voltage V_{ref}	50 V _{DC}	50 V _{DC} nominal
Output power	180 V _{AC} to 275 V _{AC}	3000 W
Efficiency peak	230 V _{AC} input, 50 V _{DC} output	$\eta_{pk} = 97.5$ percent above 18 A (30 percent of load)
Steady-state V_{out} ripple	230 V _{AC} input, 50 V _{DC} output	$ \Delta V_{out} $ less than 200 mV _{pk-pk}
Power factor and THD	180 V _{AC} to 275 V _{AC}	EN/IEC 61000-3-2 and EN 60555-2
Input UVLO	175 V _{AC} on to 170 V _{AC} off	Digital hysteresis window comparator
Output UVLO, OVLO	$V_{ref} \pm 3$ V	Shut-down and latch
Load transient	5 A \leftrightarrow 30 A, 1 A/ μ s	$ \Delta V_{out} $ less than 1 V _{pk}
	30 A \leftrightarrow 60 A, 1 A/ μ s	
Over current protection	63 to 70 A	Shut-down and resume
	More than 70 A	Shut-down and latch
	Output terminals in short-circuit	Detection within switching period Shut-down and latch
ORing		Hot insertion/removal
Front-to-back air cooling		Intenally controlled variable-speed fan
Hold-up time		0 V for 20 ms

It is worth mentioning the very high efficiency requirements, where the peak efficiency should exceed 97.5 percent at some point between 40 percent and 100 percent of the rated load. Moreover, the efficiency shall be above 96.5 percent from 40 percent to 100 percent of the load, and above 94 percent between 10 percent to 30 percent of the load. Therefore, a typical efficiency curve of a compliant PSU will look somewhat similar to the plotted curves in **Figure 2**.

The board at a glance

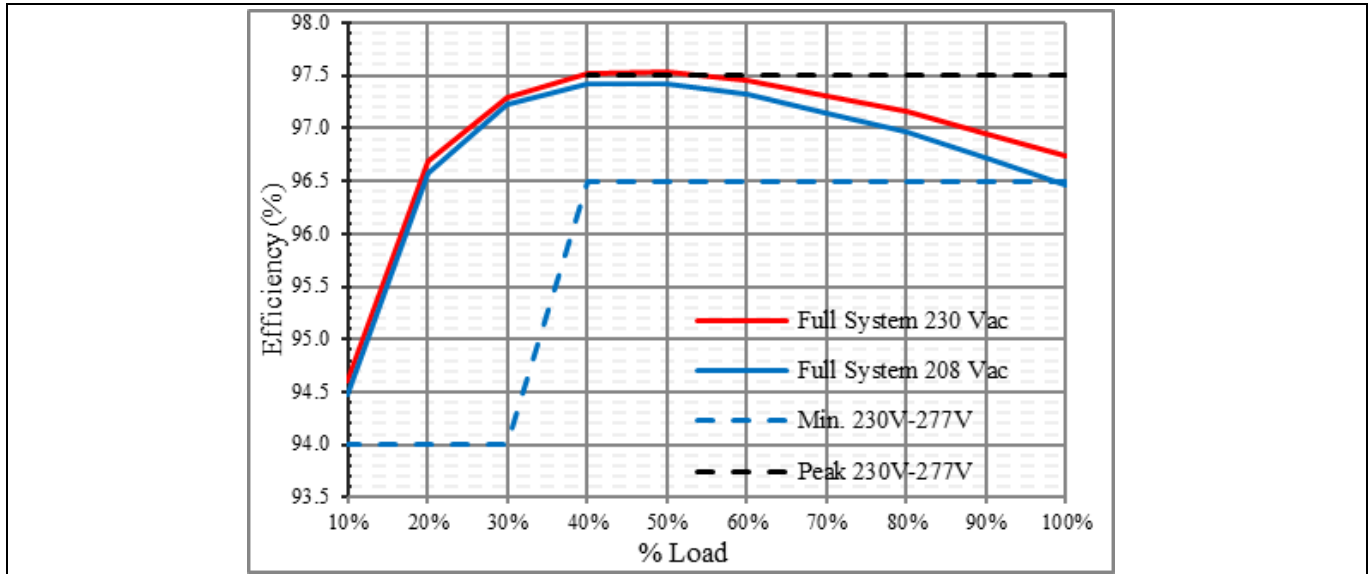


Figure 2 OCP rectifier V3 efficiency requirements at 230 V_{AC} and estimated efficiency curve of a compliant PSU

1.2 Block diagram

The PSU comprises two stages: a front-end bridgeless totem pole AC-DC converter, which provides PFC and THD, followed by a half-bridge LLC DC-DC converter that provides safety isolation and a tightly regulated output.

The control of the totem pole AC-DC converter is implemented with a XMC1404 Infineon microcontroller, which includes PFC, THD, voltage regulation, input overcurrent protection (OCP), overvoltage protection (OVP), undervoltage protection (UVP), undervoltage lockout (UVLO), soft-start, SR control, adaptive dead-times (boosting half-bridge) and serial communication interface. Further details about the digital control implementation and additional functionalities of the totem pole control with the XMC1400 family can be found in [3].

The control of the half-bridge LLC is implemented with a XMC4200 Infineon microcontroller, which includes voltage regulation functionality, burst-mode operation, output OCP, OVP, UVP, UVLO, soft-start, SR control, adaptive dead-times (bridge and SRs) and serial communication interface. Further details about the digital control implementation and additional functionalities of the LLC control with the XMC4000 family can be found in [4].

Figure 3 shows a very simplified diagram of the PSU, including the main power semiconductor switches, and the controllers and drivers of the two main conversion stages. While the PFC controller is located at one of the input V_{AC} rails, the LLC controller is referenced to the ground of the insulated output of the complete PSU. It is worth mentioning that the totem pole PFC and the LLC controllers are communicated via UART through the safety isolation barrier thanks to a digital isolator.

The board at a glance

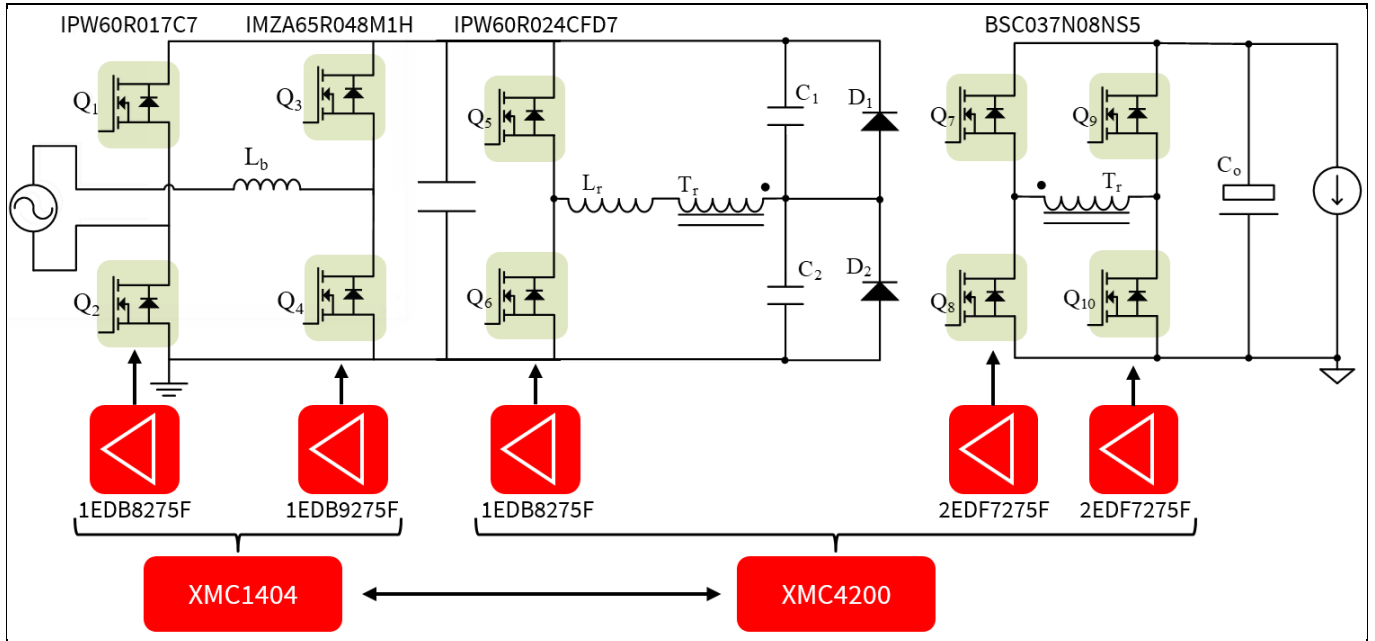


Figure 3 Simplified schematic of the prototype PSU. Front-end totem pole PFC followed by a half-bridge LLC resonant converter.

2 System and functional description

The two conforming blocks of the complete power supply can be studied and evaluated independently thanks to the Infineon evaluation boards [EVAL_3K3W_TP_PFC_SIC](#) and [EVAL_3K3W_LLC_HB_CFD7](#), which have already been released and are available for order at the Infineon website and several third-party distributors.

The EVAL_3K3W_TP_PFC_SIC is a stand-alone totem pole AC-DC converter with PFC and THD functionalities. It is an open-frame converter with an integrated internal fan. [Figure 4](#) shows a simplified circuit schematic of the EVAL_3K3W_TP_PFC_SIC.

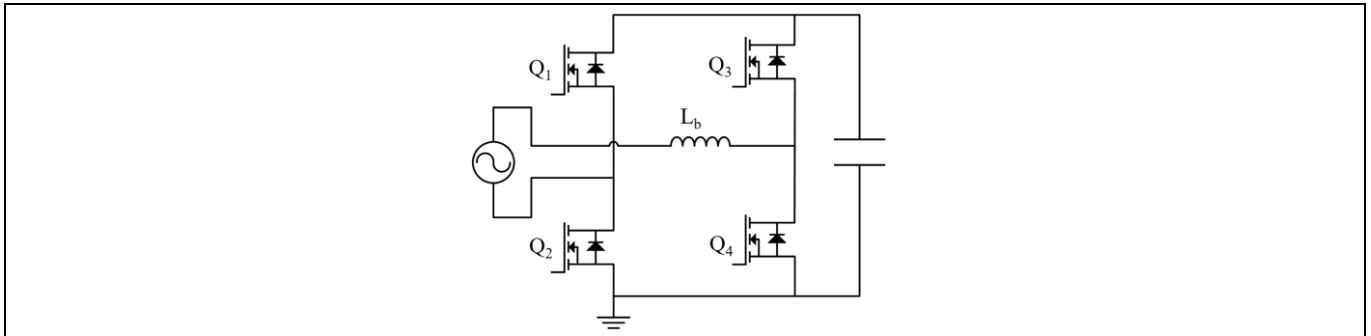


Figure 4 Simplified schematic of the totem pole AC-DC converter (EVAL_3K3W_TP_PFC_SIC)

The EVAL_3K3W_LLC_HB_CFD7 is a stand-alone LLC DC-DC converter with integrated probing points, easily replaceable primary-side switches and an oversized heatsink. It is, like the EVAL_3K3W_TP_PFC_SIC, an open-frame converter with an integrated internal fan. [Figure 5](#) shows a simplified circuit schematic of the EVAL_3K3W_LLC_HB_CFD7.

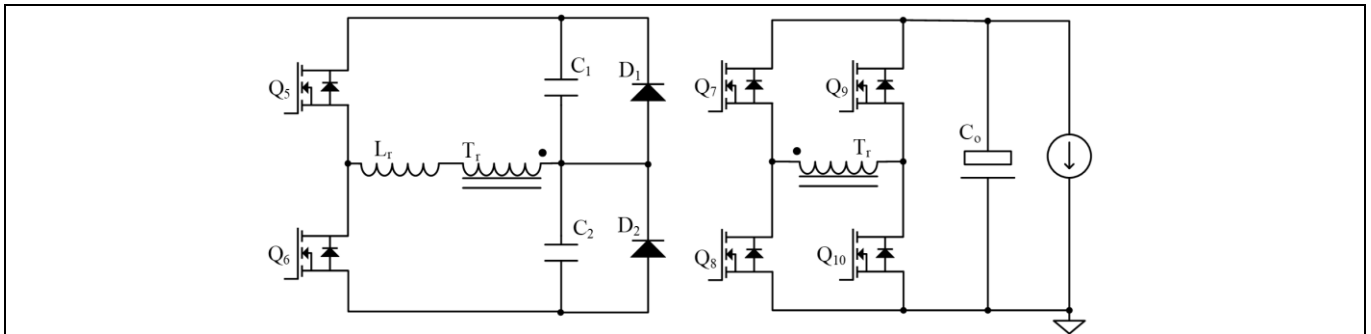


Figure 5 Simplified schematic of the half-bridge LLC DC-DC converter (EVAL_3K3W_LLC_HB_CFD7)

The two previous stand-alone blocks have been further improved and adequately modified for their integration into the complete PSU ([Figure 6](#)).

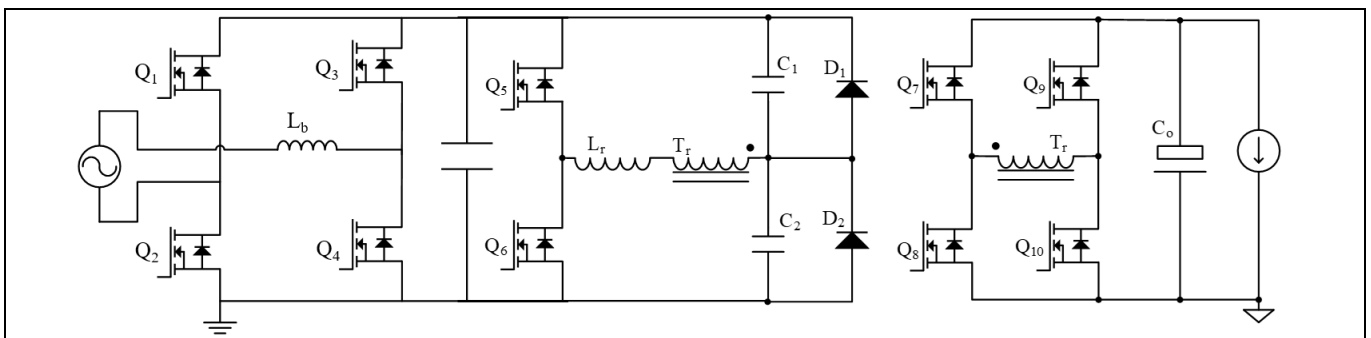


Figure 6 Simplified schematic of the EVAL_3KW_50V_PSU. Front-end totem pole PFC followed by a half-bridge LLC resonant converter.

System and functional description

2.1 Bridgeless totem pole PFC

The estimated efficiency of the redesigned totem pole PFC, part of the complete PSU, is plotted in **Figure 7**. It is worth noticing the very high peak efficiency, near 99 percent at 50 percent of the rated load.

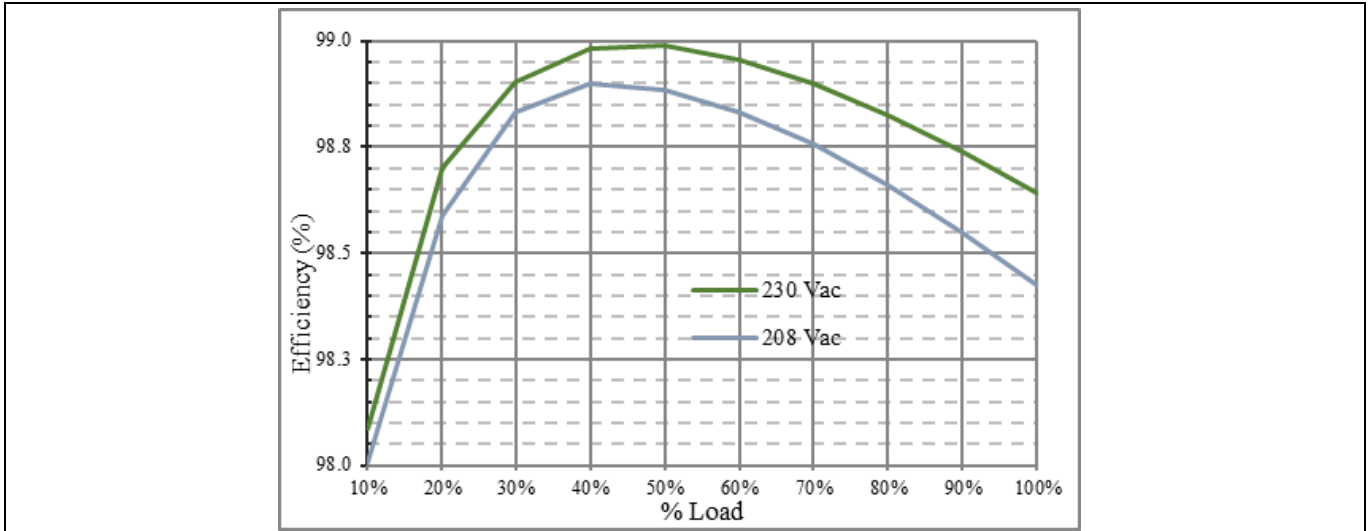


Figure 7 Estimated efficiency of the totem pole front-end AC-DC converter

The estimated overall distribution of losses of the the totem pole PFC converter at 230 V_{AC} and 50 percent of the rated load is summarized in **Figure 8**. It can be observed that the main contributors to the losses are the half-bridge boosting switches (**IMZA65R048M1H**). In a totem pole PFC the boosting switches operate mostly in hard-commutation, explaining the relatively high switching loss. However, thanks to the small parasitic capacitances of the CoolSiC™ devices and the high switching speed achievable with the 4-pin packages, the converter can still achieve very high performance. On the other hand, the low temperature dependence of the CoolSiC™ $R_{DS(on)}$ reduces the conduction loss at mid and full load, and at the lowest input voltages (where the conduction loss dominates) [5].

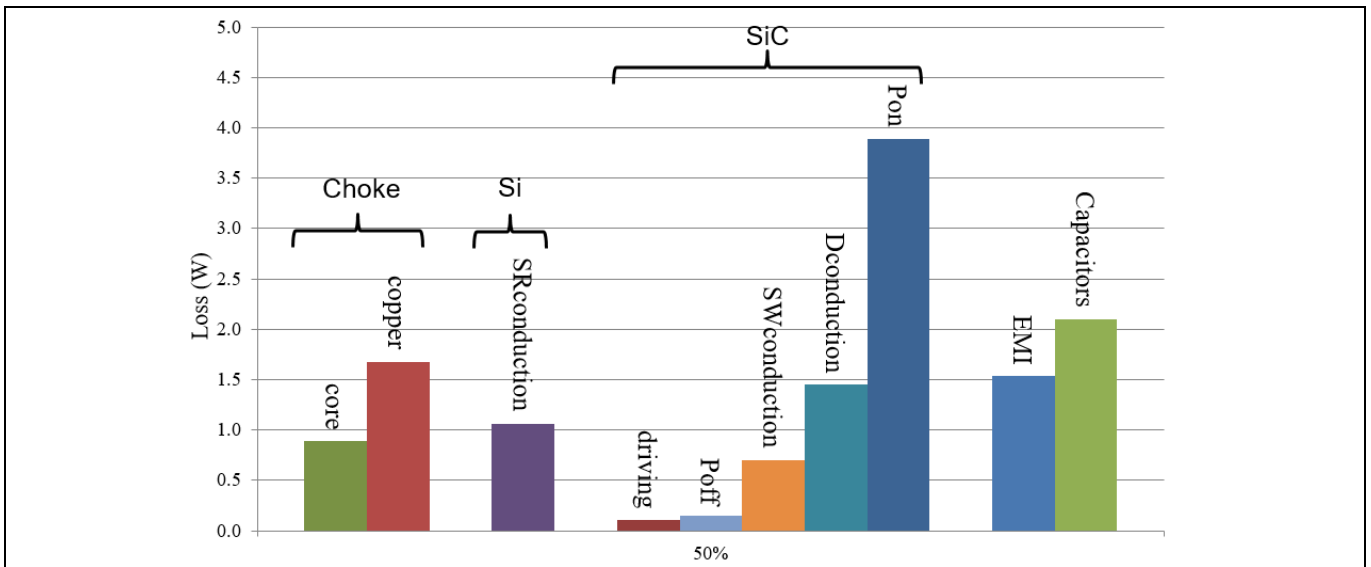


Figure 8 Estimated overall distribution of loss in the totem pole PFC at 230 V_{AC} and 50 percent of the load

System and functional description

2.1.1 Totem pole PFC magnetics

The other main contributors to the losses to consider in the design of the totem pole AC-DC converter are the main inductor and the EMI filter. The main inductor of this design is made of two stacked toroidal cores from Chang Sung: one CH330060GT and one CH330060GT14. The winding is made of 62 turns of AWG 15 insulated solid copper wire, with a total inductance of 539 μ H at no load, and of approximately 271 μ H at full load and 230 V_{AC} . **Figure 9** shows a simplified diagram of the recommended construction technique for the main boost inductor, in order to minimize unwanted parasitic capacitances.

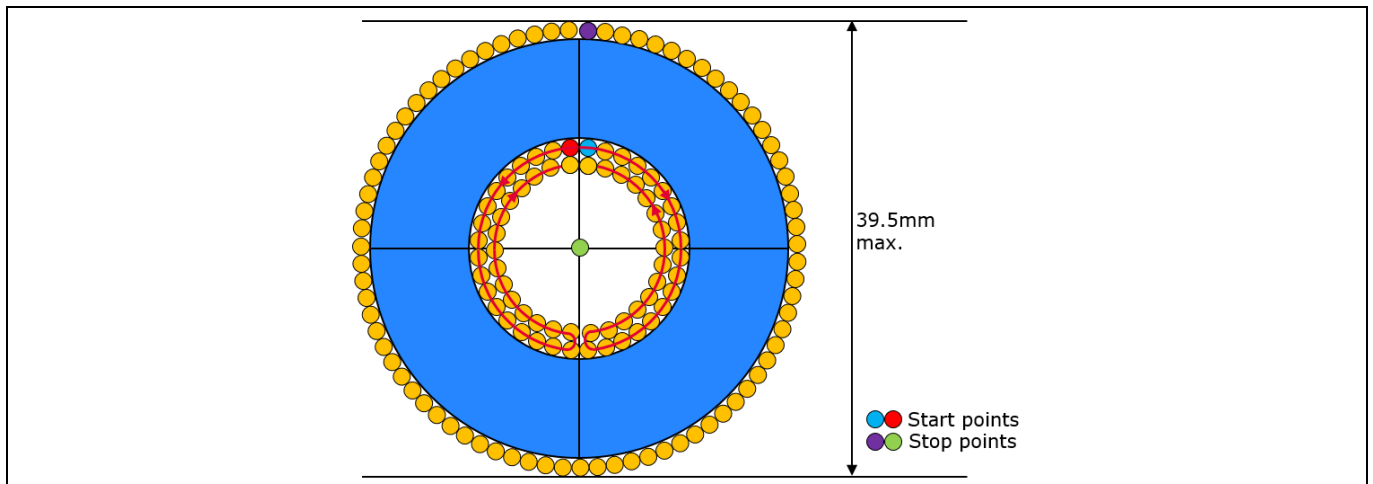


Figure 9 Simplified recommended building instructions for the main boost inductor

2.2 Half-bridge LLC

The estimated efficiency of the redesigned half-bridge LLC converter part of the complete PSU is plotted in **Figure 10**. It is worth mentioning the very high peak efficiency, near 98.5 percent at 50 percent of the rated load. Note that the overall efficiency of the complete PSU is the result of multiplying the separate efficiencies of the conforming blocks, and is necessarily lower than any of them separately. However, some of the loss contributions are shared between the two blocks (e.g., auxiliary bias) and therefore, the resulting overall efficiency is still expected to fall within the target specifications.

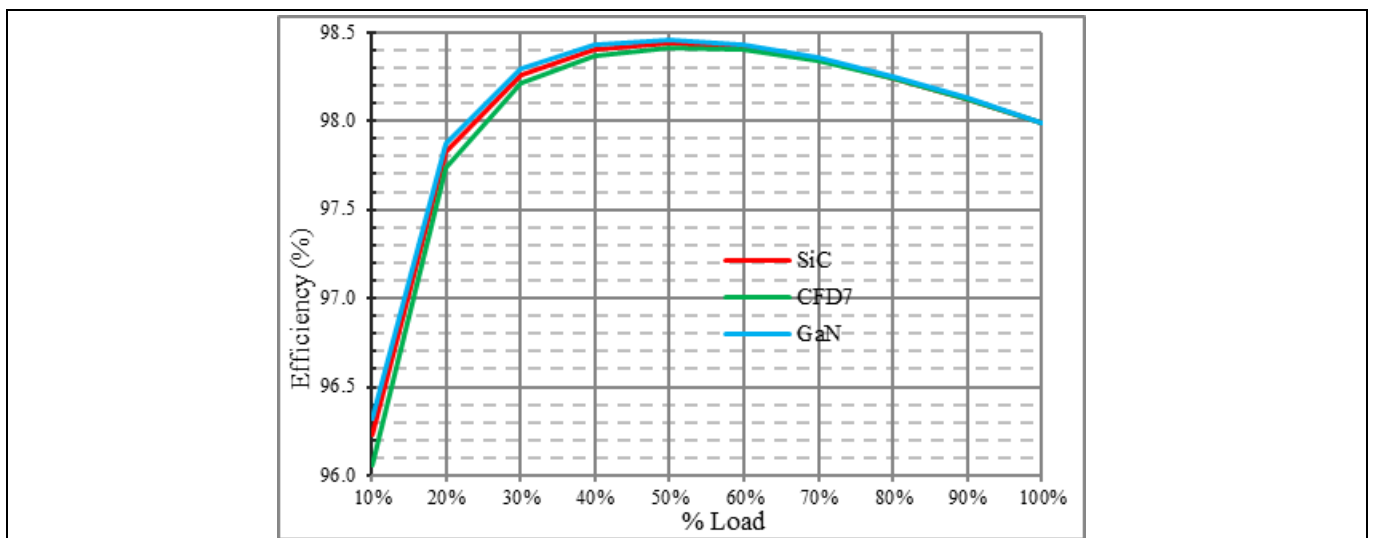


Figure 10 Estimated efficiency of the back-end LLC DC-DC converter

System and functional description

The estimated overall distribution of losses of the LLC DC-DC converter at 410 V_{DC} and 50 percent of the rated load is summarized in **Figure 11**. It can be observed that the main contributors to losses are the main transformer, followed by the SRs and the primary-side half-bridge MOSFETs. Moreover, it is worth highlighting that the switching and driving losses comprise a large portion of the total losses, and therefore the optimal series resonant frequency of this converter was found to be a relatively low 93 kHz. On the other hand, the analysis shows that even at this low switching frequency the wide-bandgap (WBG) alternatives provide improved efficiency, especially noticeable at mid and light loads.

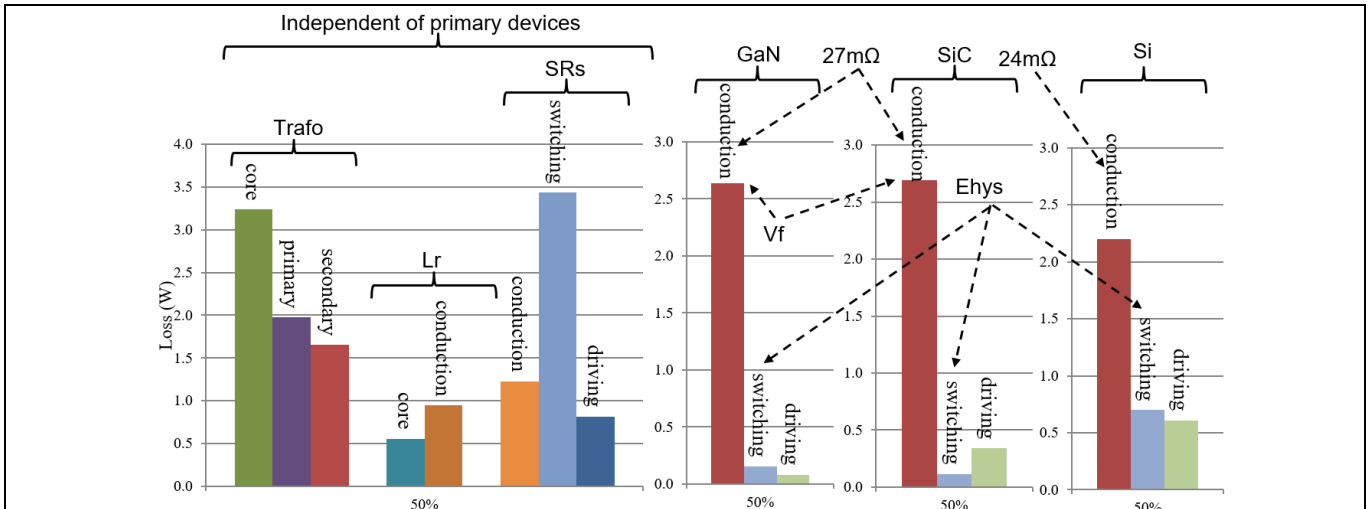


Figure 11 Estimated overall distribution of loss of the back-end LLC DC-DC converter at 50 percent load

2.2.1 Half-bridge LLC magnetics

The resonant tank of the half-bridge LLC series-parallel resonant converter comprises two equivalent inductors and one equivalent capacitor (hence its name). However, one of the advantages of this topology is that it is possible to realize the series resonant inductor (L_r) by the leakage of the main transformer, and the parallel resonant inductor (L_m) by the magnetizing inductance of the main transformer. Nevertheless, that integration approach constrains the design and compromises the performance of the converter. Therefore, in the PSU object of this work the series inductor (L_r) and the parallel inductor (L_m) are realized as discrete components, although L_m is integrated within the same structure of the main transformer.

Figure 12 shows a simplified view of the construction of the series inductor (L_r). L_r is built with a PC95 PQ35/13 DG core and a PQ135 core from TDK. The distributed gap helps reduce the losses caused by the stray magnetic fields in the winding itself and the surrounding conductors (in the main board and the chassis). Moreover, a spacer maintains the windings away from three of the gaps.

The winding is made of six turns of Litz wire with 245 strands of 0.1 mm diameter.

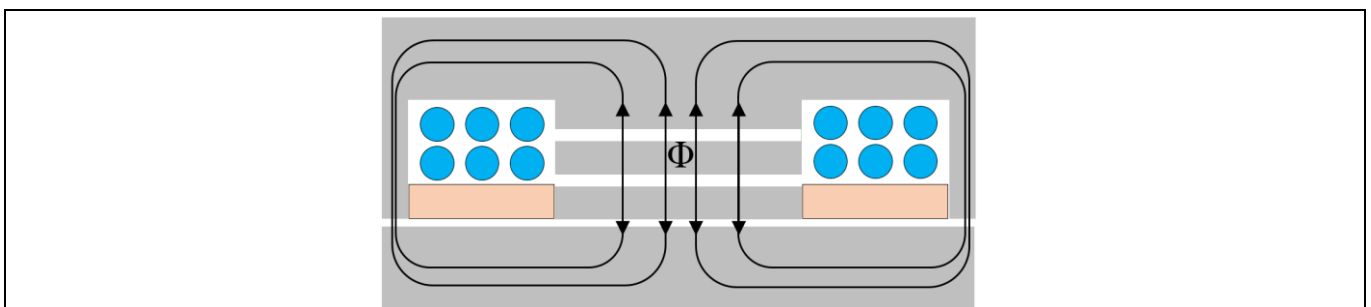


Figure 12 Simplified construction of the series resonant inductor of the LLC DC-DC converter

System and functional description

Figure 13 shows a simplified view of the construction of the parallel inductor (L_m) and the main transformer. The parallel inductor is built with a PC95 PQ35/28 core from TDK, while the main transformer is built with two PC95 PQ135/23 cores from TDK. The L_m is stacked on top of the main transformer and wound in the same direction as the primary-side winding. As a result of this, the flux in part of the volume is effectively cancelled and the total core loss is partly reduced. On the other hand, the magnetizing inductance of the main transformer can be made arbitrarily high, which contributes to the reduction of proximity loss and other loss caused by stray magnetic fields.

The winding of the L_m is made of 16 turns of Litz wire with 512 strands of 0.05 mm diameter. The main transformer windings are made of planar copper conductors built-in independent PCBs for the primary and for the secondary. The proposed construction is highly flexible and modular. The proposed interleaving realized in the PSU is demonstrated in **Figure 13** and **Figure 14**. It is worth mentioning that the transformer turn ratio is 16 to 4. Each of the primary-side winding PCBs (in blue in **Figure 13**) comprises eight turns while each of the secondary-side winding PCBs (in green in **Figure 13**) comprises four turns.

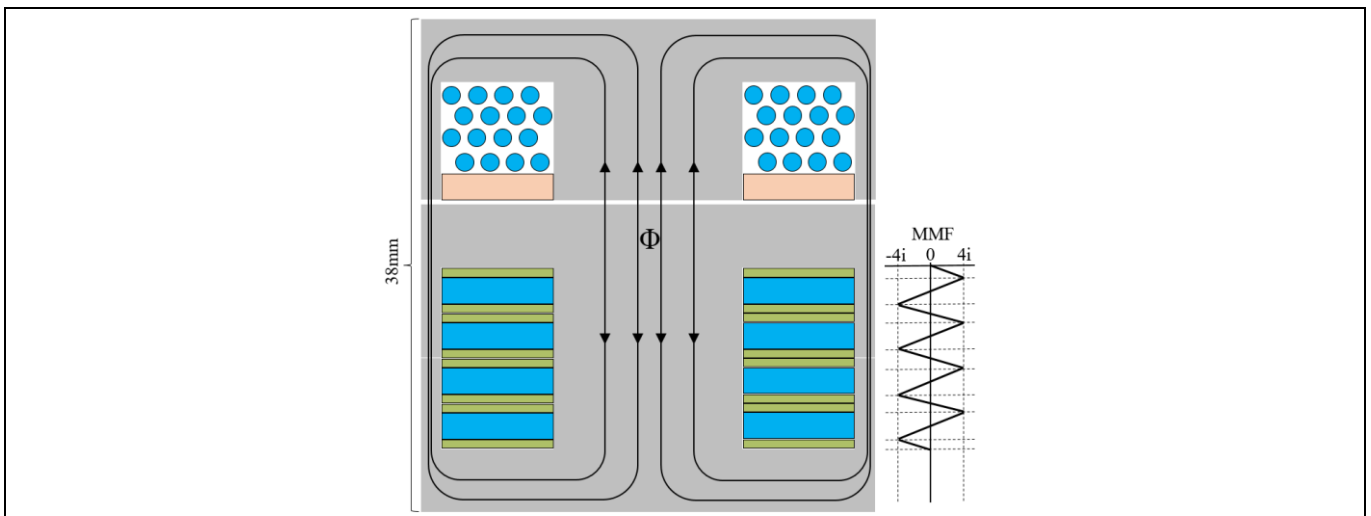


Figure 13 Simplified construction of the integrated transformer plus the parallel resonant inductor of the LLC DC-DC converter

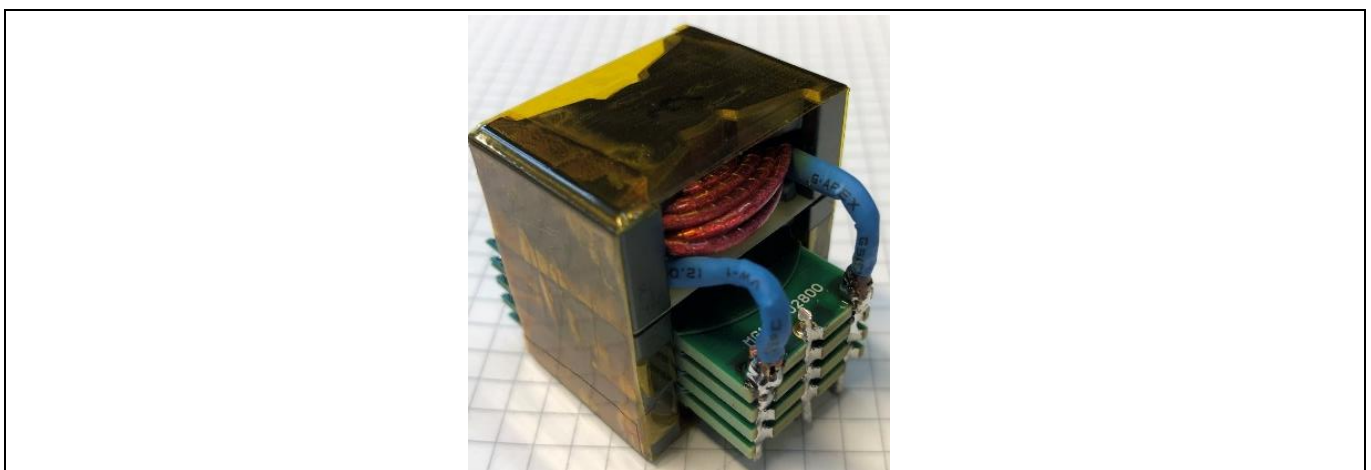


Figure 14 Photo of the assembled integrated structure of the transformer plus the parallel resonant inductor

Due to the height limitation of the PSU (40 mm) the main board needs to be cut out to accommodate the height of the integrated L_m plus the main transformer structure (approximately 38 mm).

3 Experimental results

This section is a summary of the main experimental results of each of the conforming blocks separately (totem pole PFC and half-bridge LLC), and of the complete PSU.

3.1 Totem pole PFC

In the bridgeless totem pole AC-DC converter the boosting half-bridge operates mostly in hard-commutation. Therefore, the switching loss depends on the switching speed of the devices, i.e. the longer the overlap of voltage and current, the higher the loss. For this purpose, the 4-pin TO-247 package with Kelvin source connection helps by removing the negative feedback caused by the power source during the switching transients and making the device switch faster. On the other hand, the switching speed of the devices shall be controlled to avoid excessive drain voltage overshoot and gate ringing, which can be achieved with a properly dimensioned external gate resistor.

Figure 15 is an example of the drain voltage overshoot and gate ringing in the boosting half-bridge of the totem pole PFC. Both the drain voltage and the gate voltage have been measured referenced to the Kelvin source connection. It can be observed that the maximum drain overshoot is 487 V, well within the rated limits of the devices.

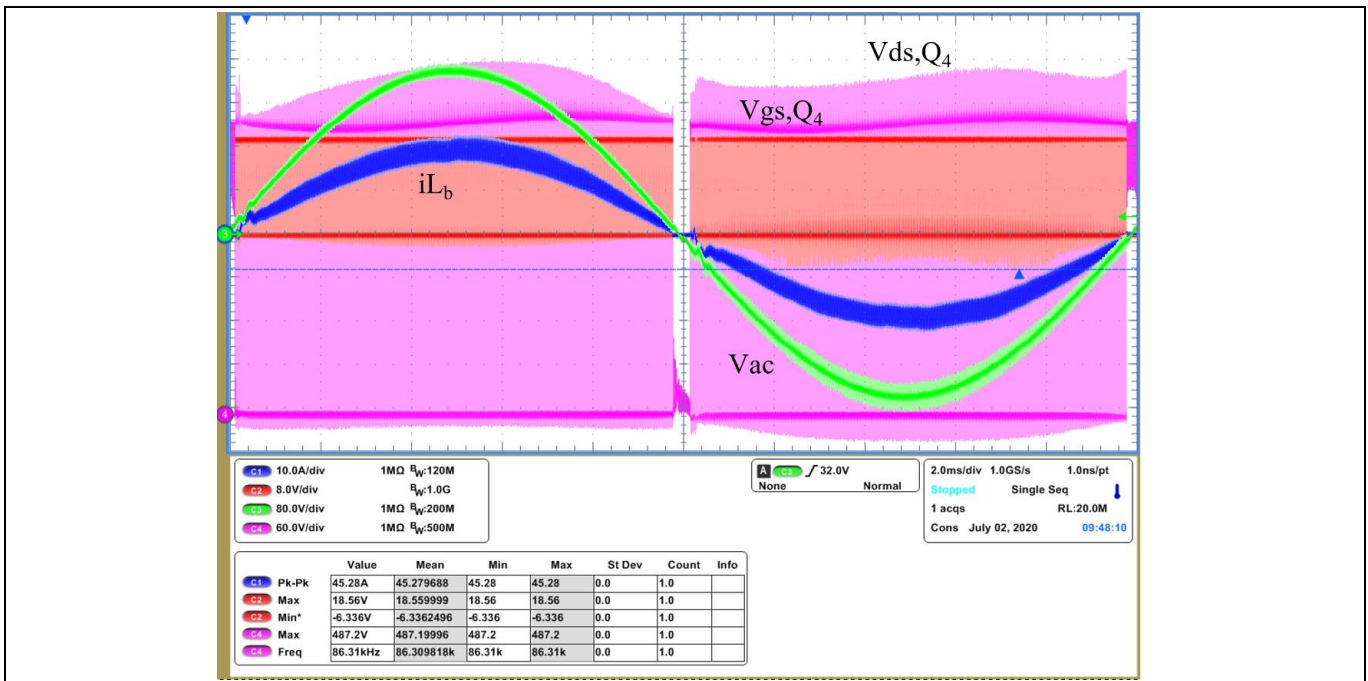


Figure 15 PFC drain voltage overshoot and gate ringing at full load

3.1.1 Boost diode operation

The devices in the boosting half-bridge of the totem pole AC-DC converter operate alternately as the boost converter diode and the boost converter switch. The modes alternate at twice the V_{AC} frequency.

The switching transients are clearly different while the device operates as a diode or as a switch. During operation as a diode, the device is zero voltage switched (ZVS) both at turn-on and turn-off. After the opposite boost switch turns off, the inductor current freewheels to the intrinsic body diode of the boost diode device. After an idle time (dead-time) the device switches on in ZVS (Figure 16) and the current passes through the channel of the device (instead of its intrinsic body diode).

Experimental results

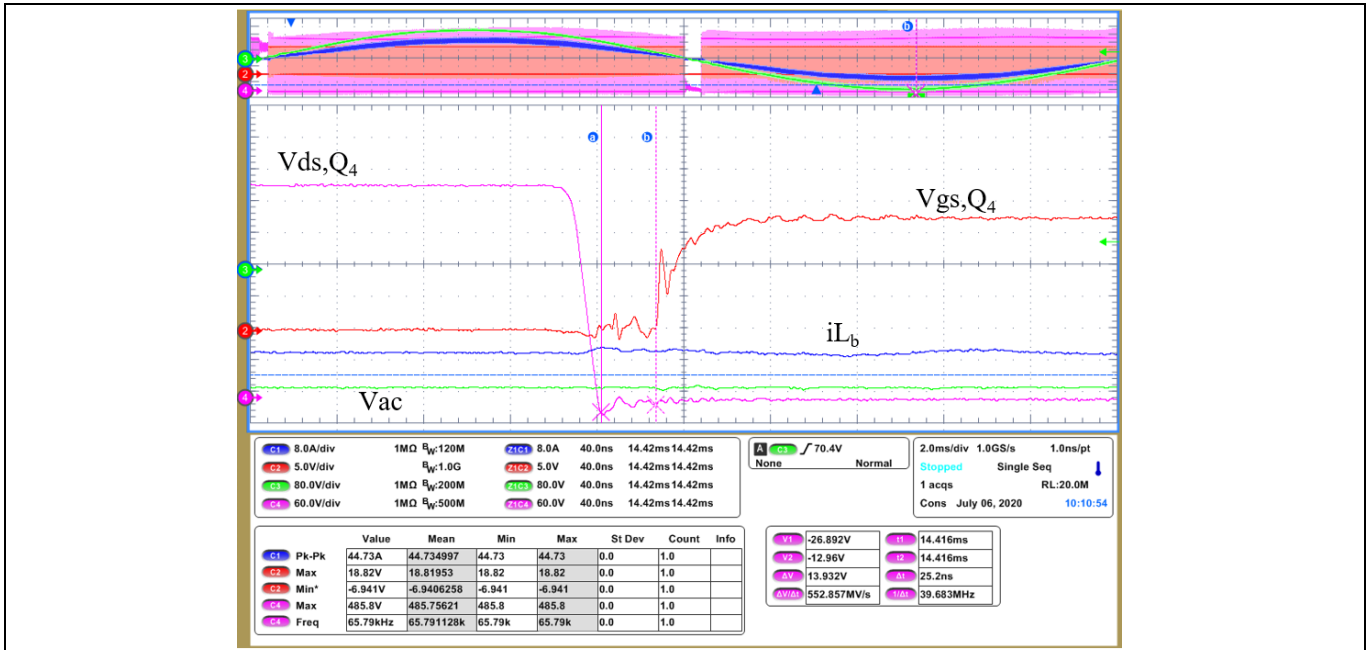


Figure 16 ZVS switch-on of the boost diode

After the boost diode device switches off in ZVS, the current continues to freewheel through its intrinsic body diode. After the corresponding idle time (dead-time) the opposite boost switch hard-switches on and hard-commutates the boost diode, which can be identified by instant where the V_{DS} rises in Figure 17.

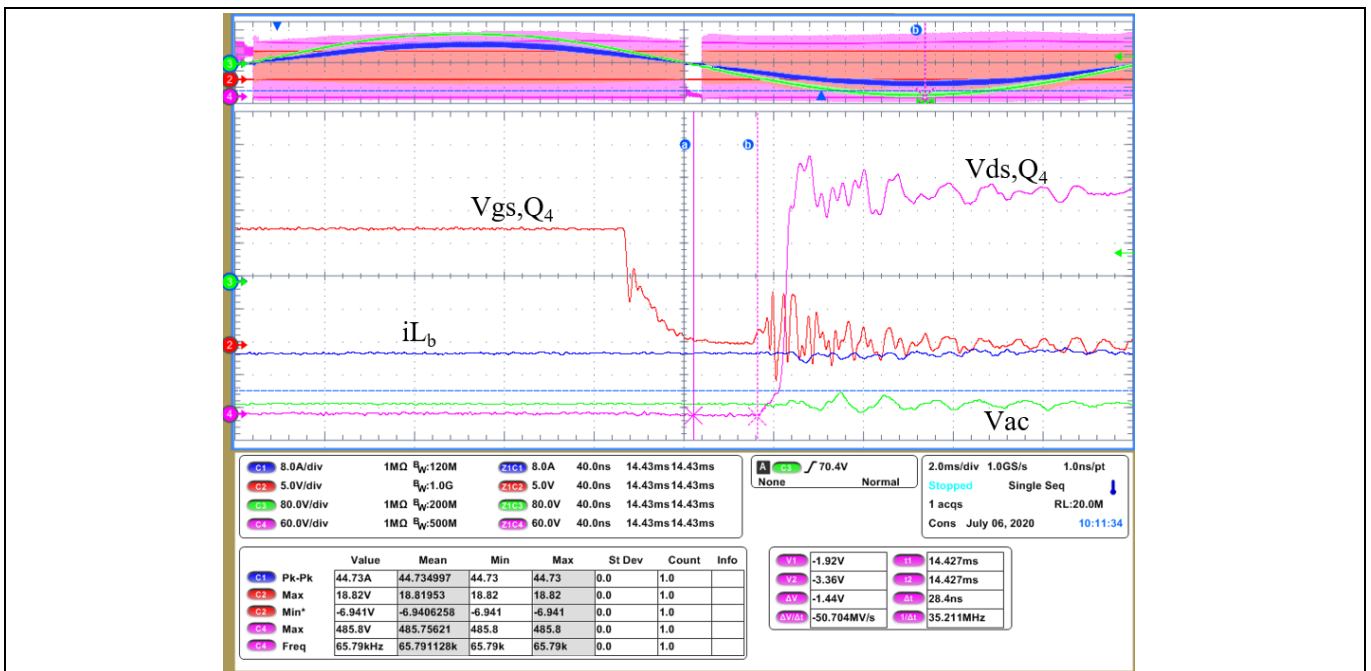


Figure 17 ZVS switch-off of the boost diode followed by its hard-commutation caused by the hard-switching on of the opposite boost switch

3.1.2 Boost switch operation

Unlike the diode operation, the boost switch operation is hard-switched during most of the V_{AC} cycle and along most of the load range. Only when the current ripple through the inductor is at least twice as large as the average current can both the diode and the switch operate in ZVS.

Server and data center 3 kW 50 V PSU

EVAL_3KW_50V_PSU

Experimental results

Figure 18 shows a hard-switched turn-off transition of the boost switch. During the hard-switched turn-off transition the dv/dt and the V_{DS} overshoot can be controlled with an external gate resistor.

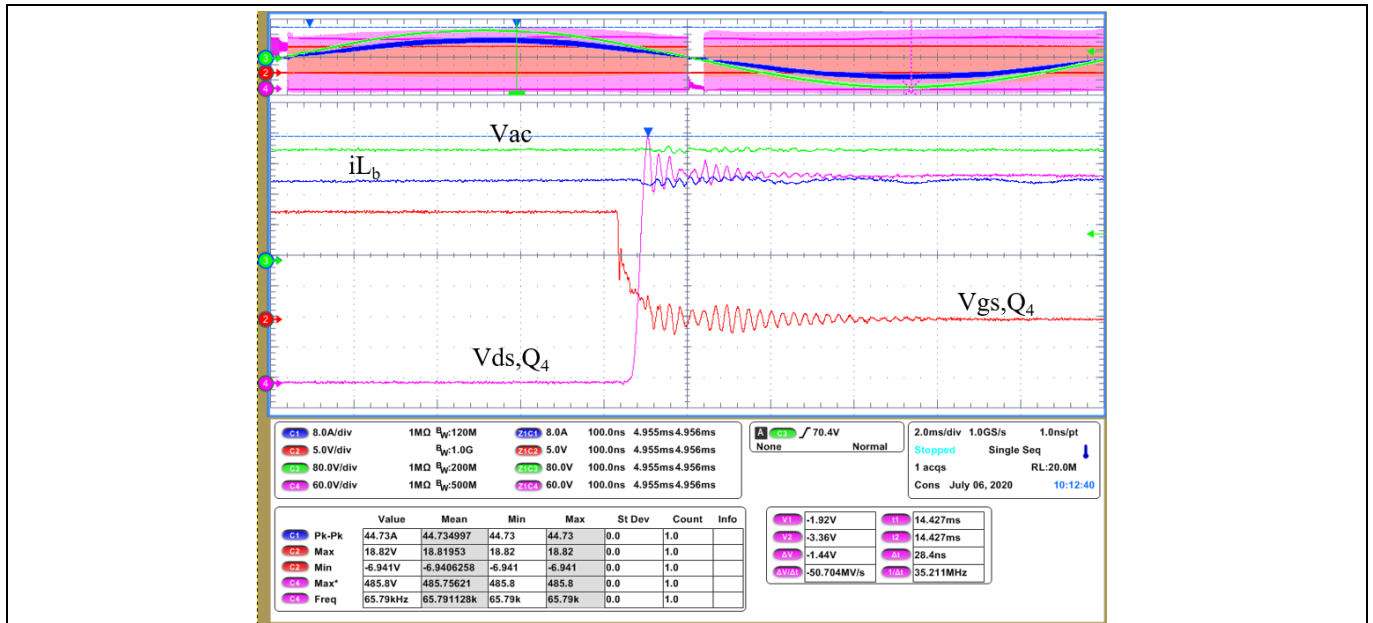


Figure 18 Hard-switched turn-off of the boost switch

Figure 19 shows a hard-switched turn-on transition of the boost switch (hard-commutation of the opposite boost diode). The device is not only hard-switching turn-on but also hard-commutating the opposite diode, hence the need to use low Q_{rr} devices in the boosting half-bridge of the totem pole AC-DC converter.

As during the hard-switched turn-off transition, the dv/dt and the gate ringing can be controlled with an external gate resistor.

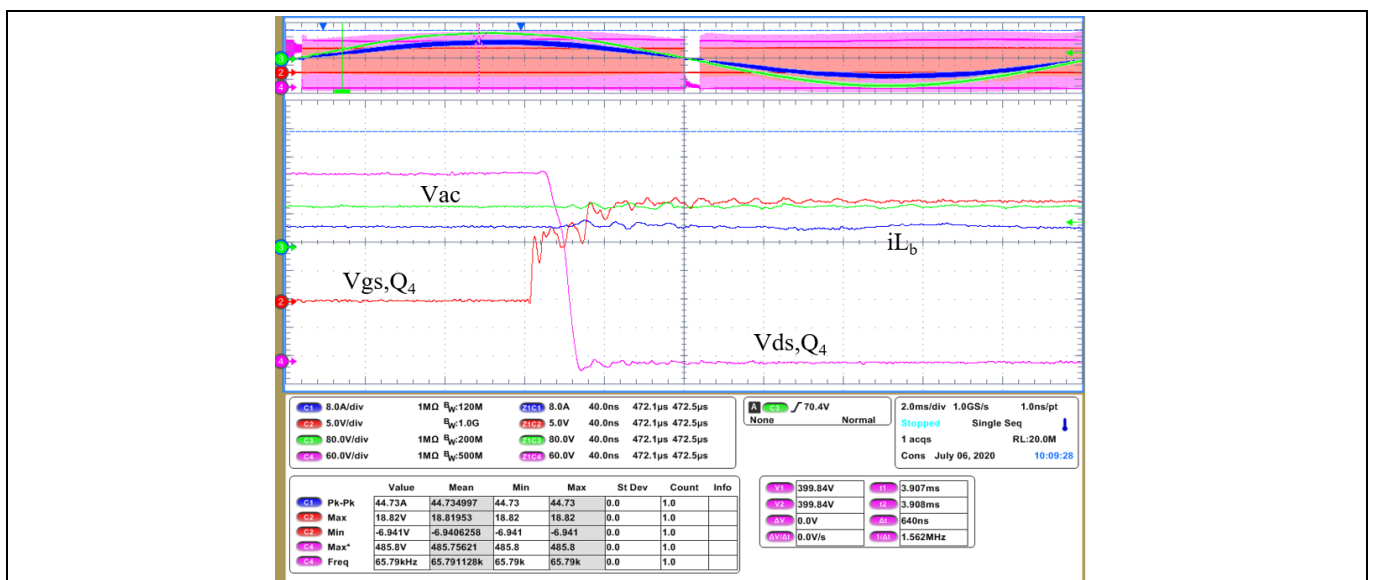


Figure 19 Hard-switched turn-on of the boost switch and hard-commutation of the boost diode

3.1.3 SRs polarity detection

Totem pole rectification can be implemented with diodes or with SRs. The SRs are only switching at twice the V_{AC} frequency, and they are normally zero current switched (ZCS). Therefore, the SRs can be implemented with very low-ohmic devices for best performance of the converter.

The SRs are normally switched around the V_{AC} crossing, with a certain idle window near the zero crossing (**Figure 20**). Moreover, this window is preferably narrow for best THD.

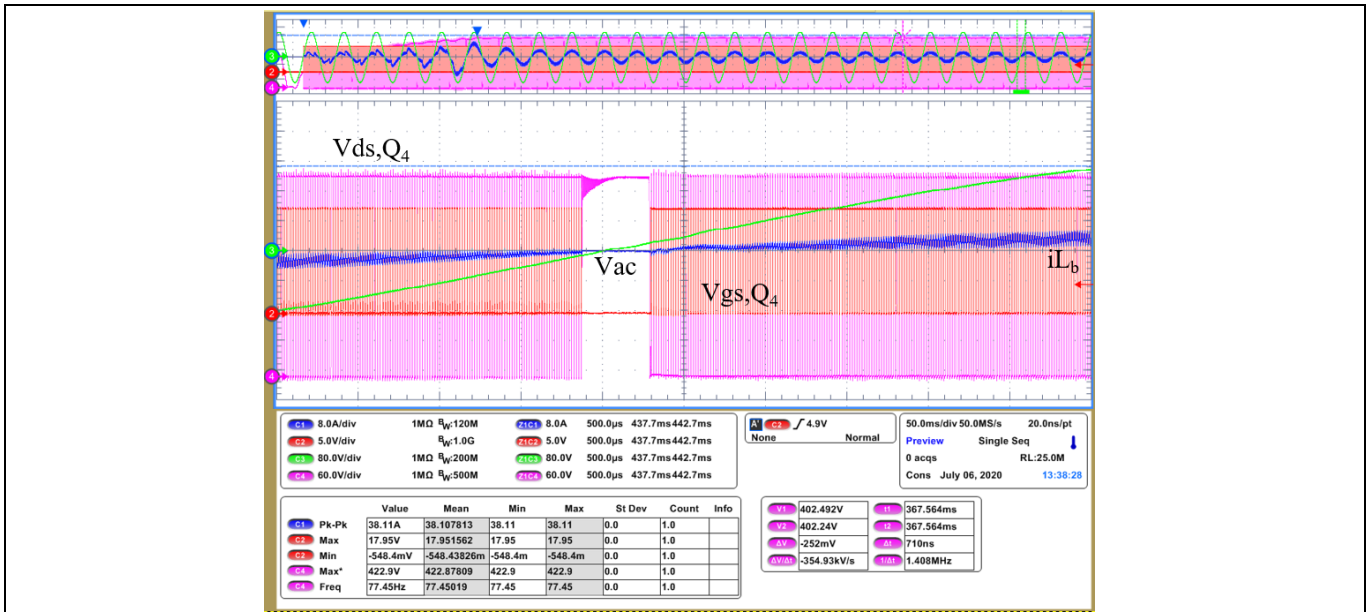


Figure 20 Detailed view of the V_{AC} zero crossing in the PFC totem pole

The implemented control can recognize an incorrect polarity detection of the SRs, turn them off and restart the next V_{AC} semi-cycle normally. In **Figure 21** it can be observed how the V_{AC} oscillation, after the V_{AC} is lost, causes the wrong polarity to be detected by the control. Nevertheless, it is noticeable that the control has recognized the wrong polarity and turns off the switches safely.

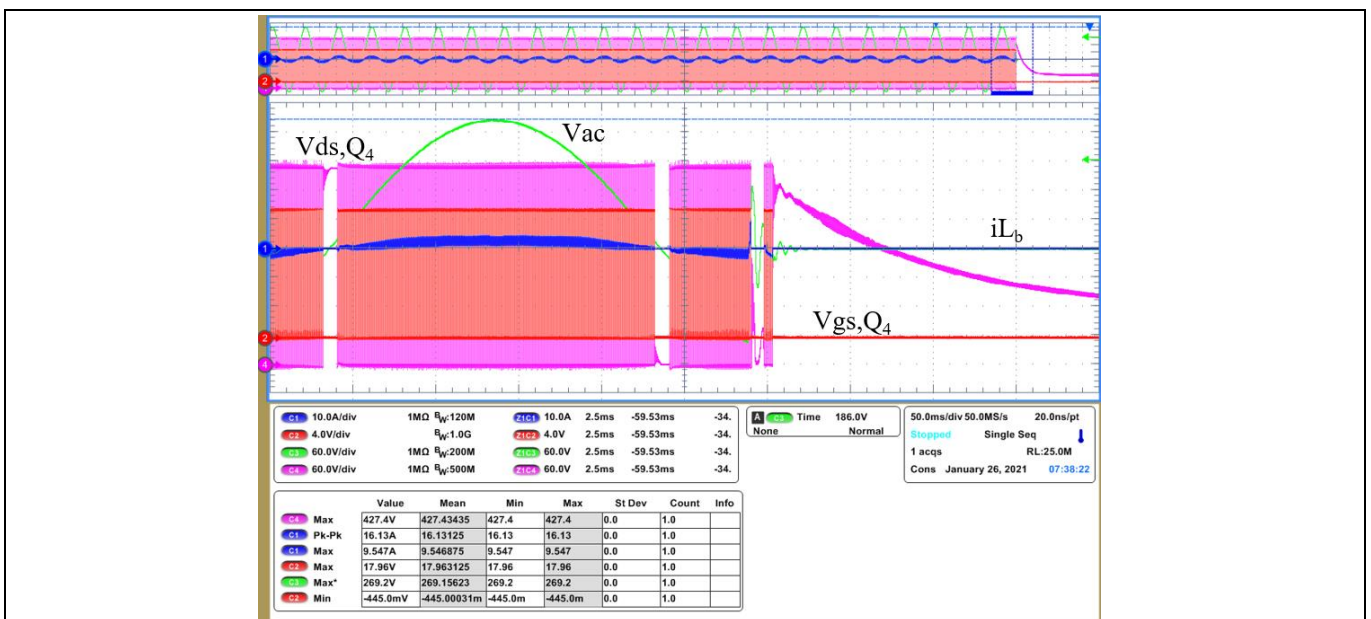


Figure 21 Filtering of V_{AC} polarity during V_{AC} loss

3.1.4 Soft-start

During soft-start the totem pole AC-DC converter has to charge up the bulk capacitance to the steady-state voltage (410 V_{DC}). At 380 V_{DC} the back-end DC-DC converter starts up and the totem pole AC-DC converter must then provide the load power plus the remaining bulk voltage charge-up.

Figure 22 shows the soft-start sequence of the totem pole PFC at 10 A load. The start-up of the back-end DC-DC converter is visible in the current of the PFC, near the end of the ramp-up of the voltage, with an increase due to the charge of the output capacitance of the DC-DC converter itself.

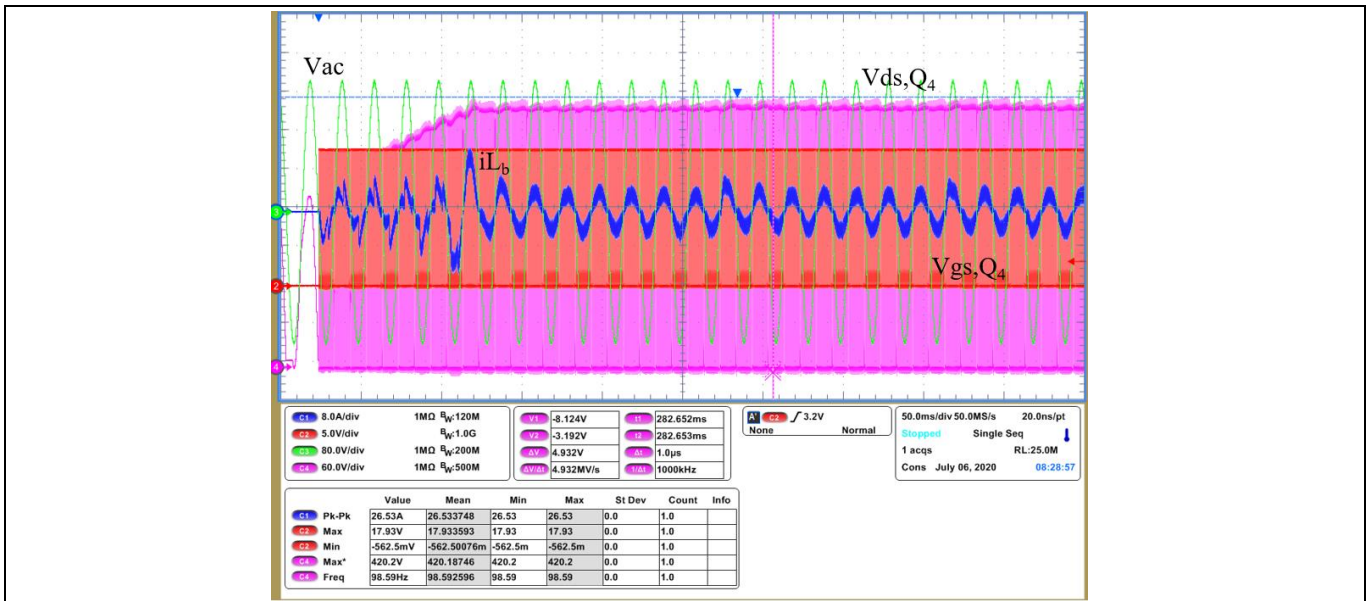


Figure 22 Soft-start sequence of the totem pole PFC at 180 V_{AC} and 10 A load

Figure 23 shows the start-up of the totem pole PFC at the minimum rated input voltage (180 V_{AC}) and at 55 A load. The start-up of the DC-DC converter can also be observed by the increase in the sinusoidal current near the end of the ramping-up of the bulk voltage, which afterward goes into steady-state at near full power.

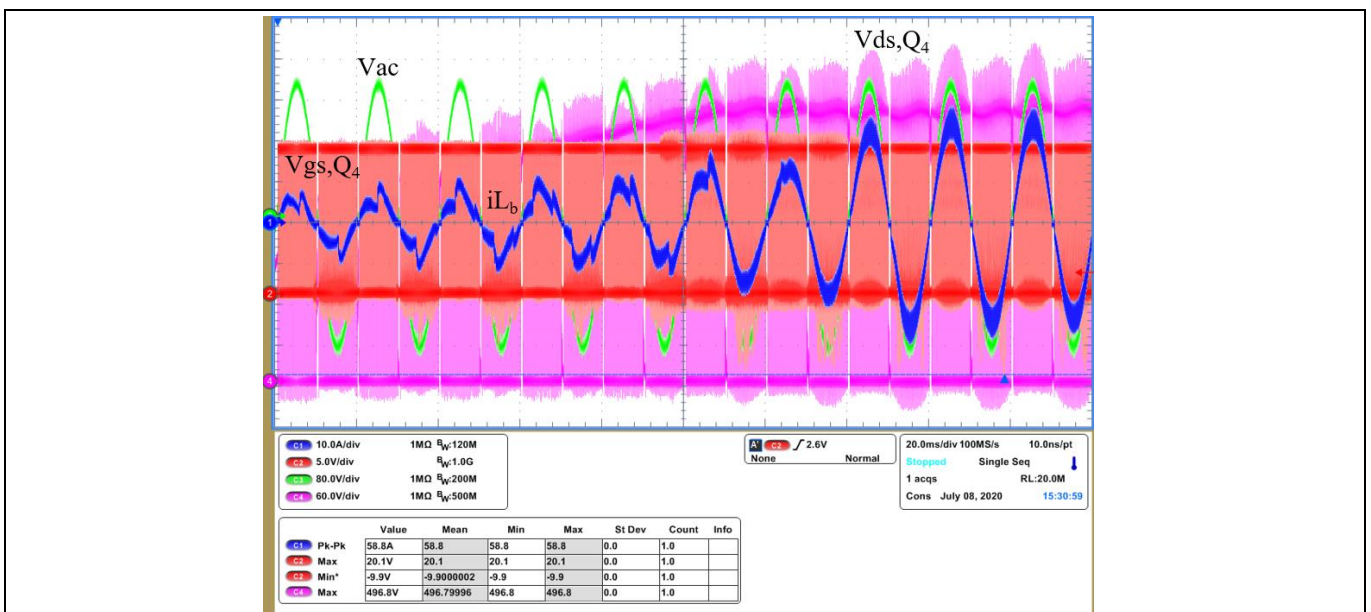


Figure 23 Soft-start sequence of the totem pole PFC at 180 V_{AC} and 55 A load

Experimental results

3.2 Half-bridge LLC

The half-bridge LLC can achieve ZVS turn-on in the primary-side half-bridge along all the load range. On the other hand, the turn-off is hard-switched. However, if the dv/dt is not limited by the device during the resonant transition, the turn-off transition becomes lossless [6]. **Figure 24** shows the ZVS turn-on and the lossless turn-off of the half-bridge LLC at 10 percent of the rated load – the lack of Miller plateau can be observed during the turn-on transition and also during the turn-off transition.

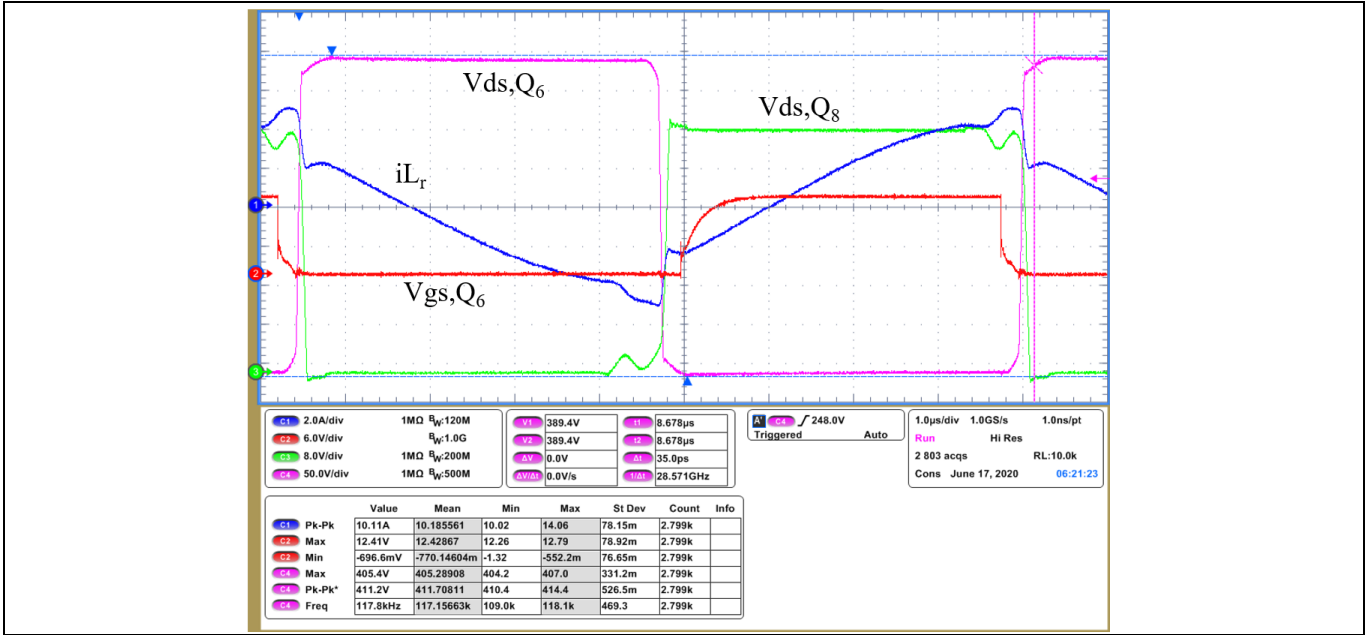


Figure 24 Full ZVS at 10 percent of the rated load

The half-bridge LLC converter operates slightly above the series resonance in nominal conditions. Therefore, it operates in buck mode, near the normalized unity gain, where the converter achieves its highest efficiency. **Figure 25** shows the primary-side reflected load current on top of the parallel inductor current. Because the main transformer magnetizing inductor is very large (approximately 1 mH) the magnetizing inductance contribution to the primary-side current can be safely ignored.

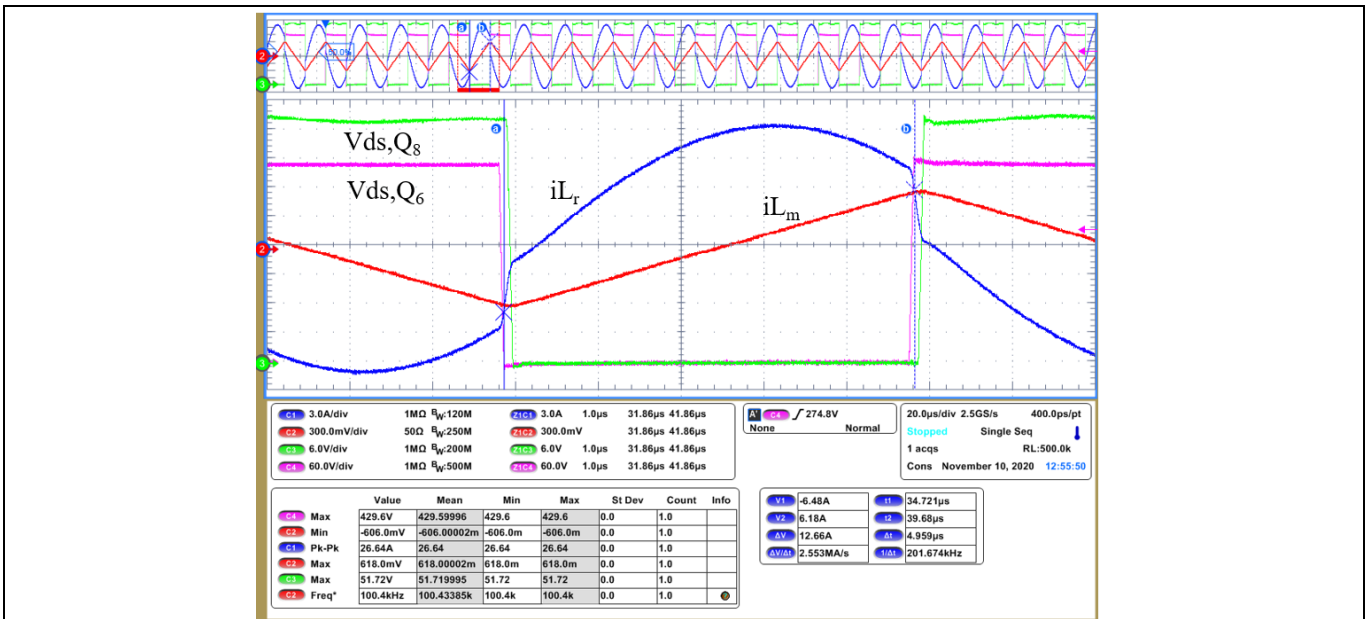


Figure 25 Steady-state operation at 50 percent of the rated load and at 410 V input voltage

Server and data center 3 kW 50 V PSU

EVAL_3KW_50V_PSU

Experimental results

The secondary-side SRs in the LLC converter are ZVS switched on and ZVS switched off. The gate driving voltage of the SRs can be observed in **Figure 26**. It should be noted that the SRs' gate driving voltage is 8.5 V to minimize the gate driving losses without much effect on their effective $R_{DS(on)}$.

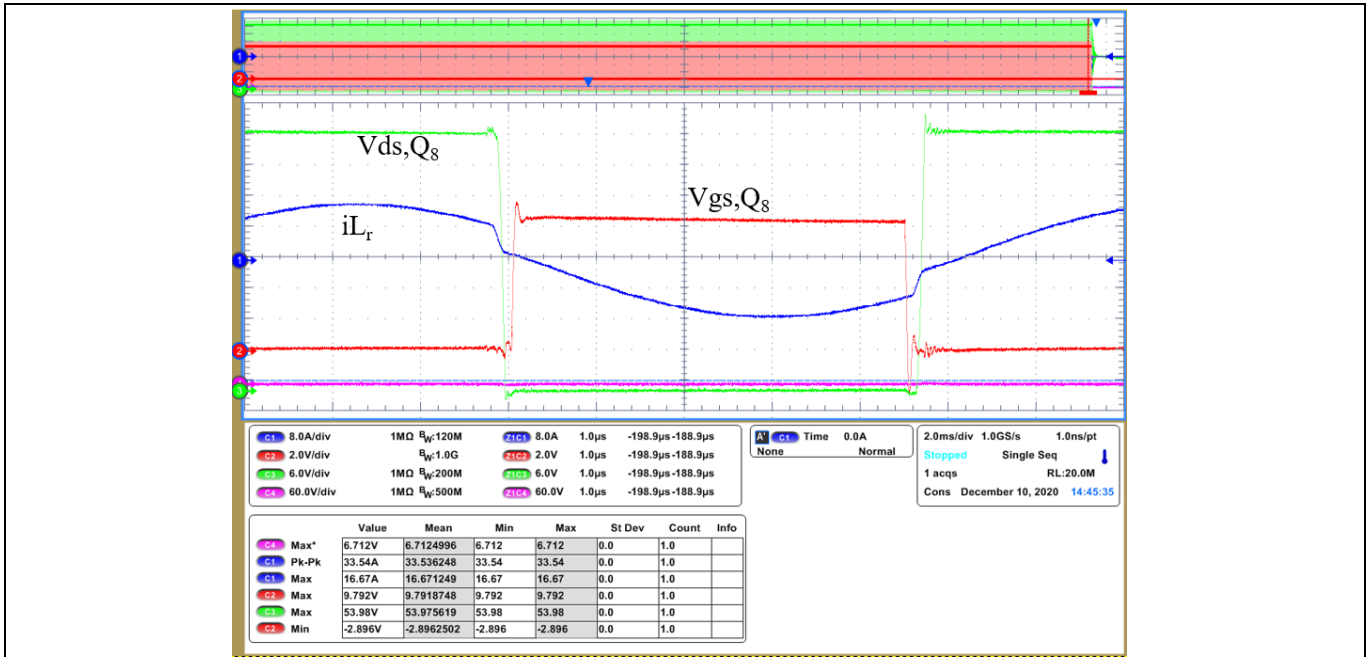


Figure 26 SRs gate driving at 40 A load and 410 V input voltage

3.2.1 ZVS switching

Figure 27 and **Figure 28** offer a more detailed view of the ZVS turn-on and the lossless hard-switched turn-off transitions of the primary-side half-bridge. Note the very low overshoot of the SRs' drain voltage, i.e. 52.64 V in **Figure 28**, well below the maximum rated voltage of the selected devices (80 V device class).

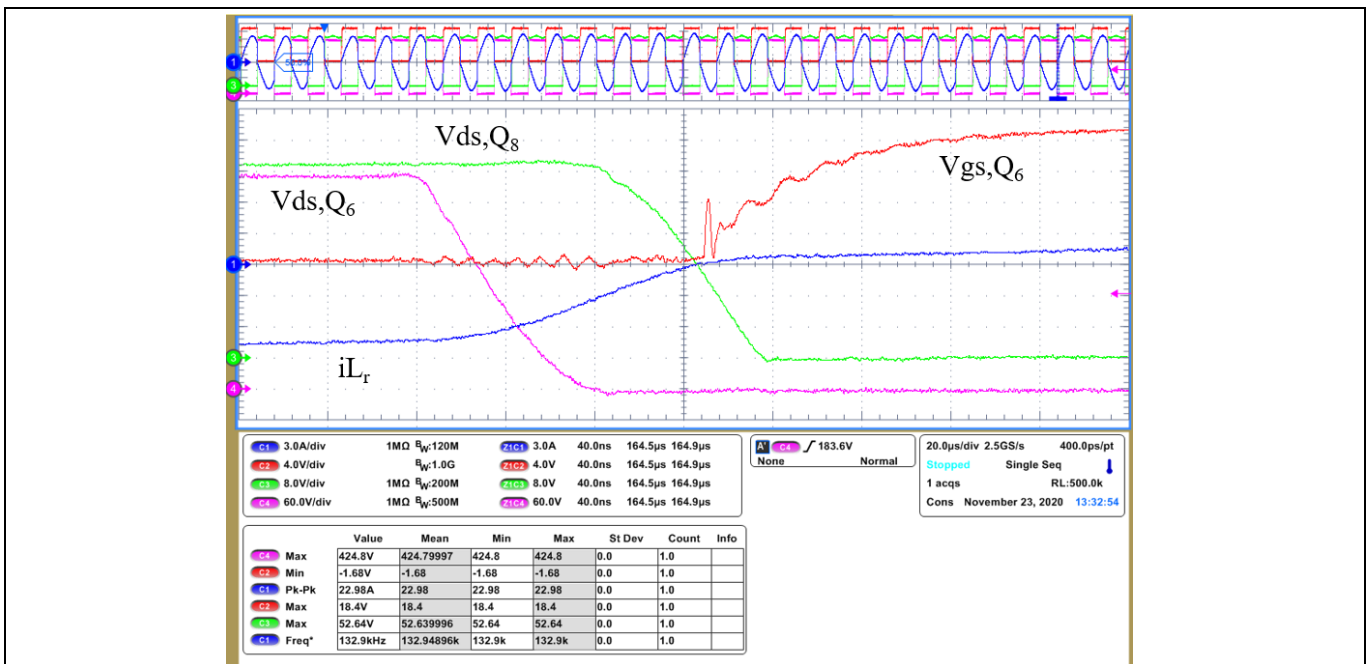


Figure 27 Detail view of the ZVS turn-on of the primary-side half-bridge

Experimental results

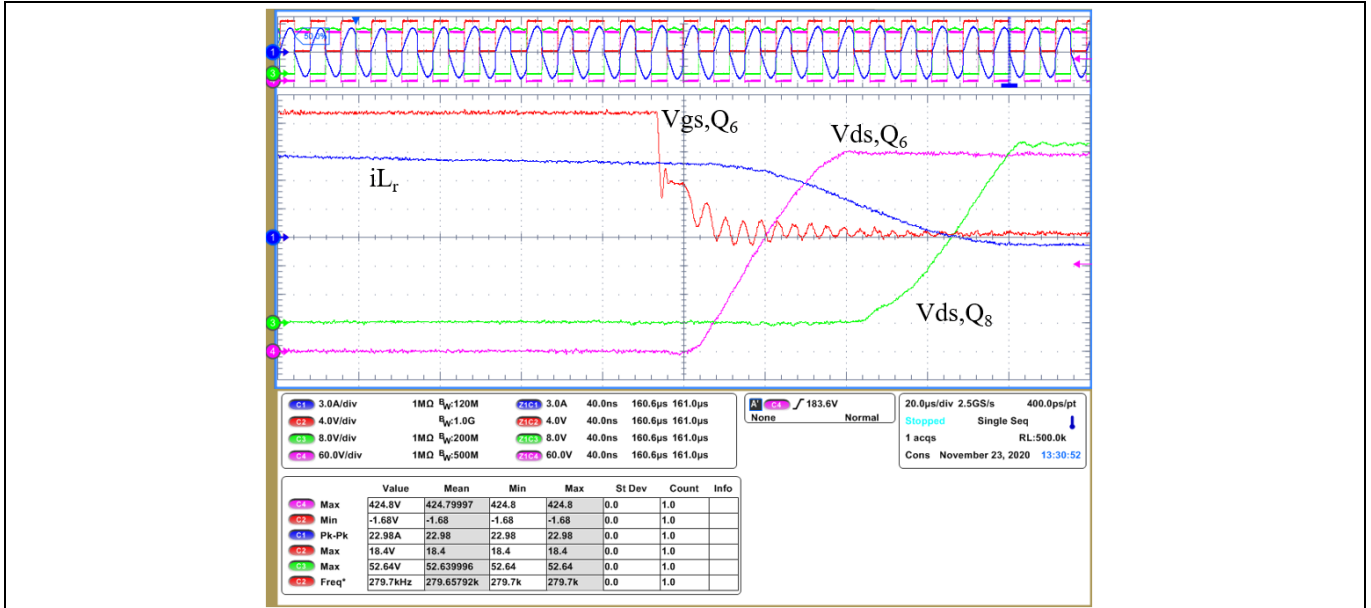


Figure 28 Detail view of the lossless hard-switched turn-off of the primary-side half-bridge

3.2.2 Soft-start

The start-up sequence is normally one of the most stressful operation modes for the semiconductor devices in the half-bridge LLC converter. During the start-up sequence the converter has to charge up the output capacitance of the converter, which causes high peak currents during the hard-switched turn-off transition. Therefore, the highest drain voltage overshoots and ringing in the gate appear during this operation mode, which can be reduced by controlling the switching speed of the devices with external gate resistors.

The monotonic rising output voltage of the converter can be observed in [Figure 29](#).

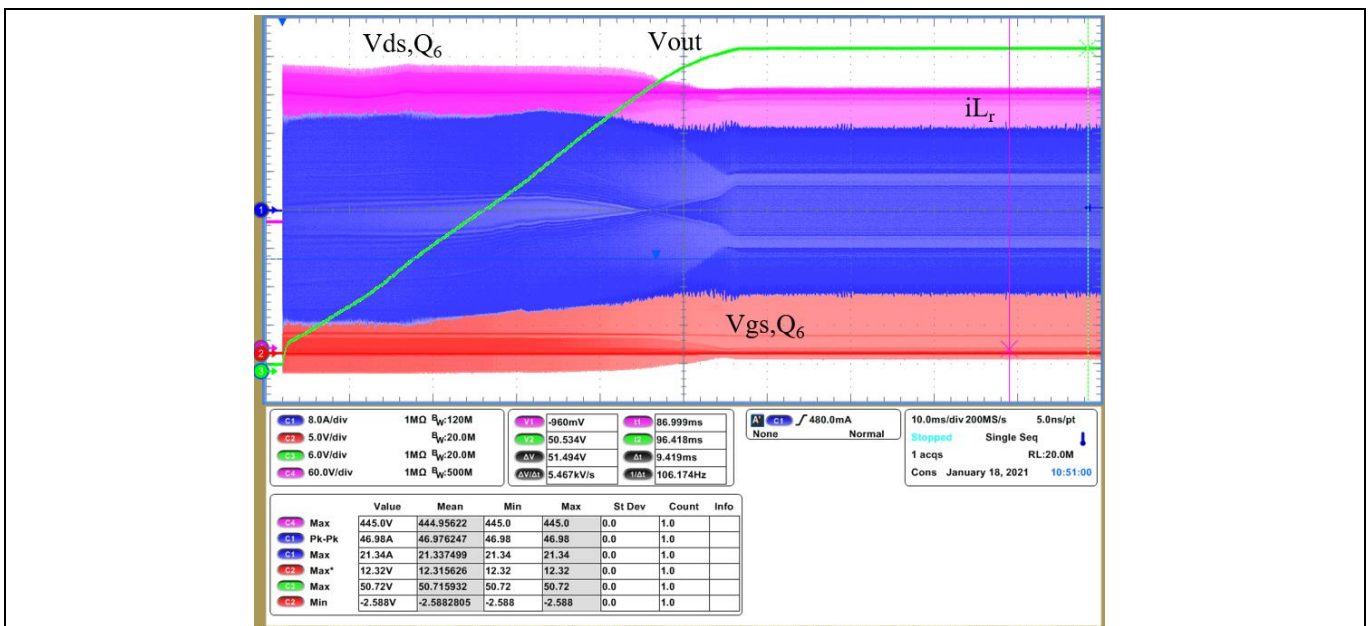


Figure 29 Soft-start sequence at 40 A load

The control of the LLC converter should ensure no hard-commutation occurs in the primary-side devices during the start-up sequence. Because the discharged output capacitors behave virtually as a short-circuit, the first pulses during the start-up sequence are at a much higher frequency ([Figure 30](#)).

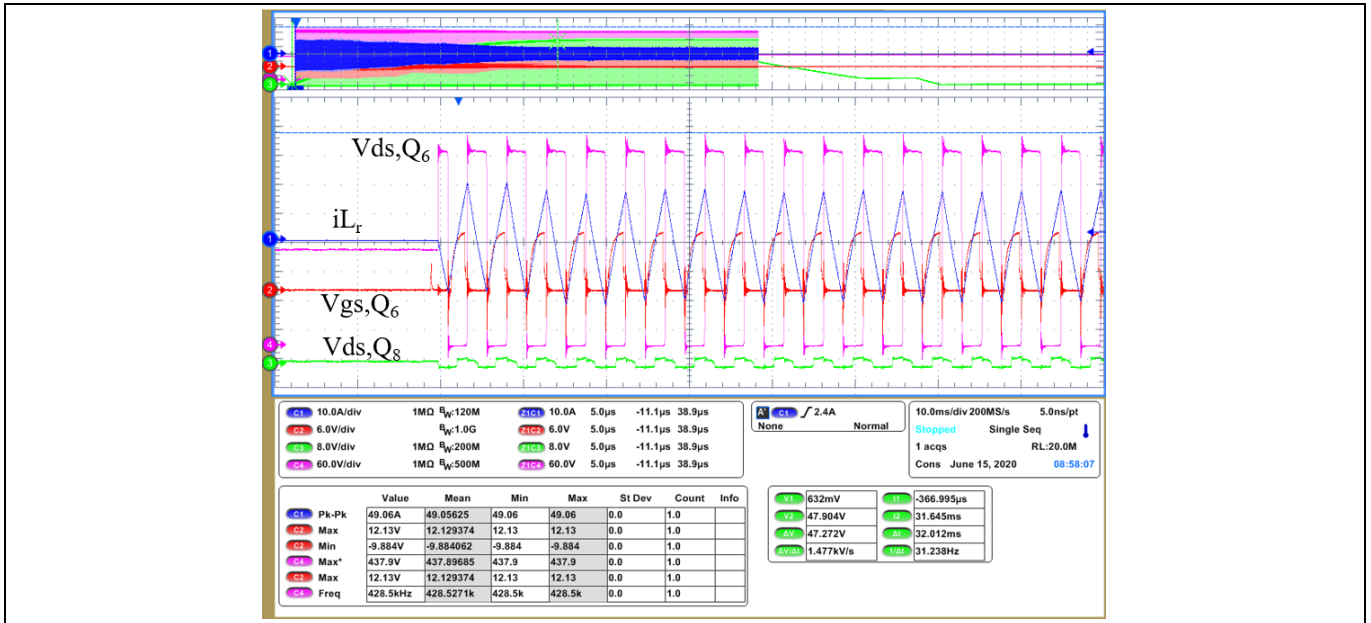


Figure 30 Detail view of the first pulses of the soft-start sequence

Because of the split-capacitor configuration of the half-bridge LLC converter, the mid-point of the primary-side half-bridge is charged up to half of the bulk voltage prior to the very first pulse. Thanks to this, the very first hard-switched turn-on pulse is only hard-switching half of the input voltage. This explains the very low overshoot seen in the first hard-switched on transition (**Figure 31**).

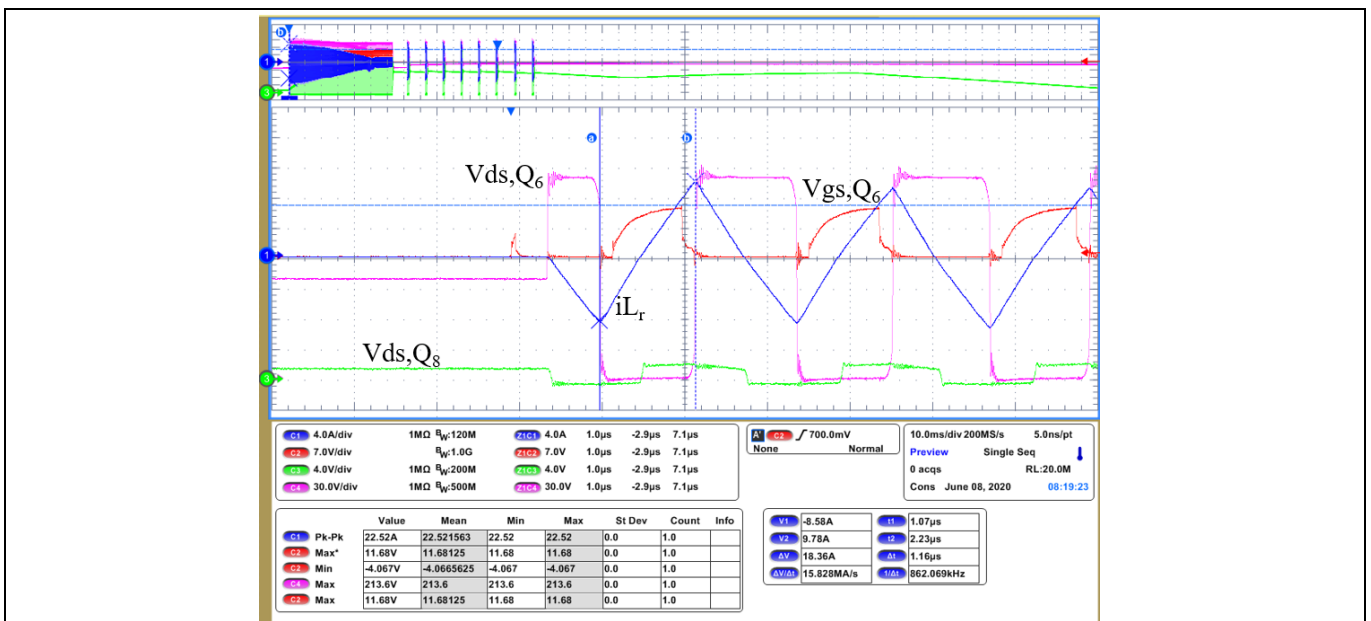


Figure 31 Detail view of the first pulses of the soft-start sequence

3.2.3 Output voltage ripple

At the output of the designed LLC converter there is an additional inductor that forms a CLC filter, which helps reduce the output voltage ripple of the converter, as well as the common-mode noise injected into the output. The high-frequency ripple is within 230 mV peak-to-peak in steady-state and at full load (**Figure 32**).

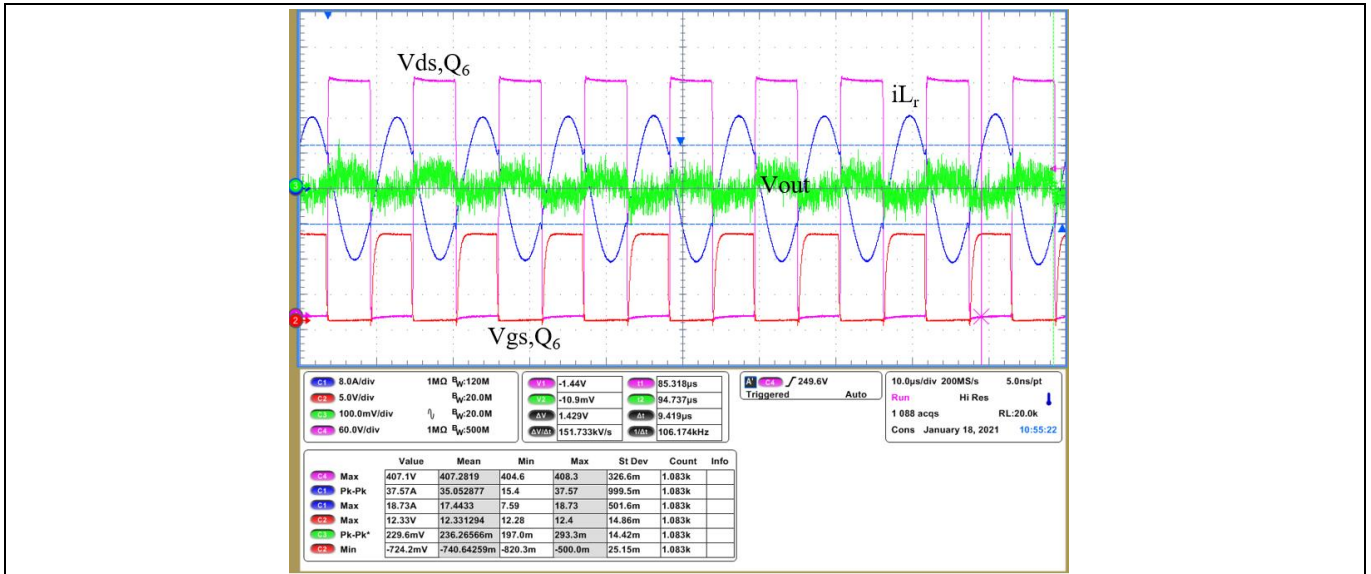


Figure 32 Output voltage ripple at full load

During the dynamic load jumps the peak-to-peak voltage variation is approximately 1.4 V for a 50 percent load jump, which falls within less than ± 2 percent of the nominal output voltage (50 V_{DC}). Moreover, the settling time is in the order of 2.5 ms (Figure 33) and with a good margin of phase, in accordance with the observable step response.

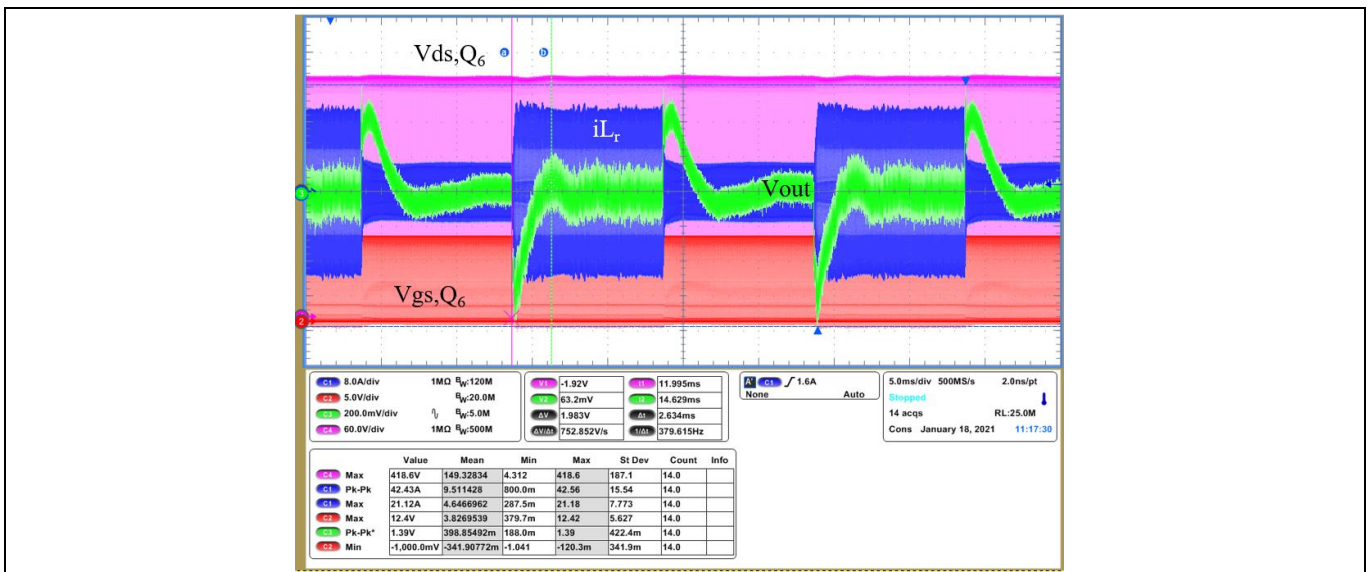


Figure 33 Dynamic load jump 10 A load to 40 A load, 1 A/ μ s, 100 Hz

3.2.4 Resonant capacitor voltage

It is well known that while the clamping diodes provide overcurrent and overload protection to the LLC converter, they also limit the maximum voltage excursion possible in the split resonant capacitors. Furthermore, as the input voltage decreases, e.g., during hold-up time, the clamping voltage decreases as well. Therefore, it should be taken into account, during the design, that the maximum available gain of the converter will be limited by the clamping diodes during the hold-up time and the resonant capacitors should be dimensioned accordingly.

Server and data center 3 kW 50 V PSU

EVAL_3KW_50V_PSU

Experimental results

Alternatively, the clamping diodes can be removed from the circuit, although other overload and overcurrent mechanisms should be then considered. **Figure 34** shows the peak-to-peak voltage excursion of the resonant capacitor being clamped when the input voltage falls down to $300 V_{DC}$.

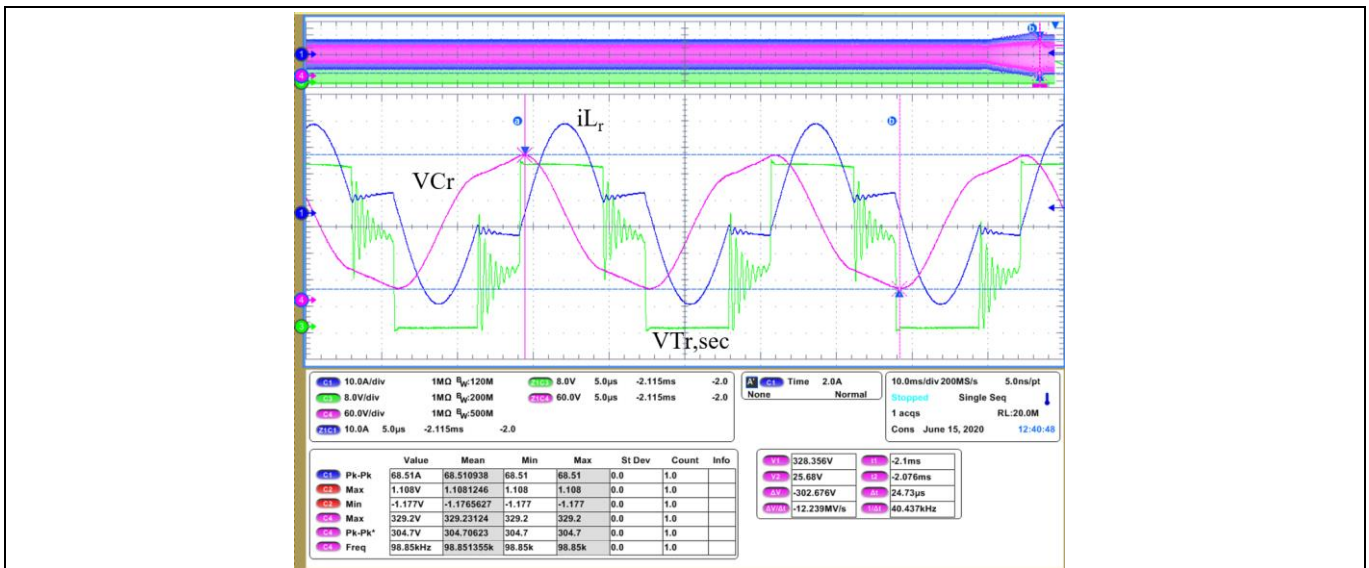


Figure 34 Clamping diodes limit the maximum V_{Cr} voltage amplitude, and therefore the gain of the converter

3.3 Power supply unit

This section provides a summary of experimental results of the complete power supply. **Figure 35** and **Figure 36** show the soft-start and brown-out sequences of the LLC integrated into the complete power supply. Unlike in **Figure 29**, the superimposed ripple in the bulk voltage due to the PFC operation can be seen.

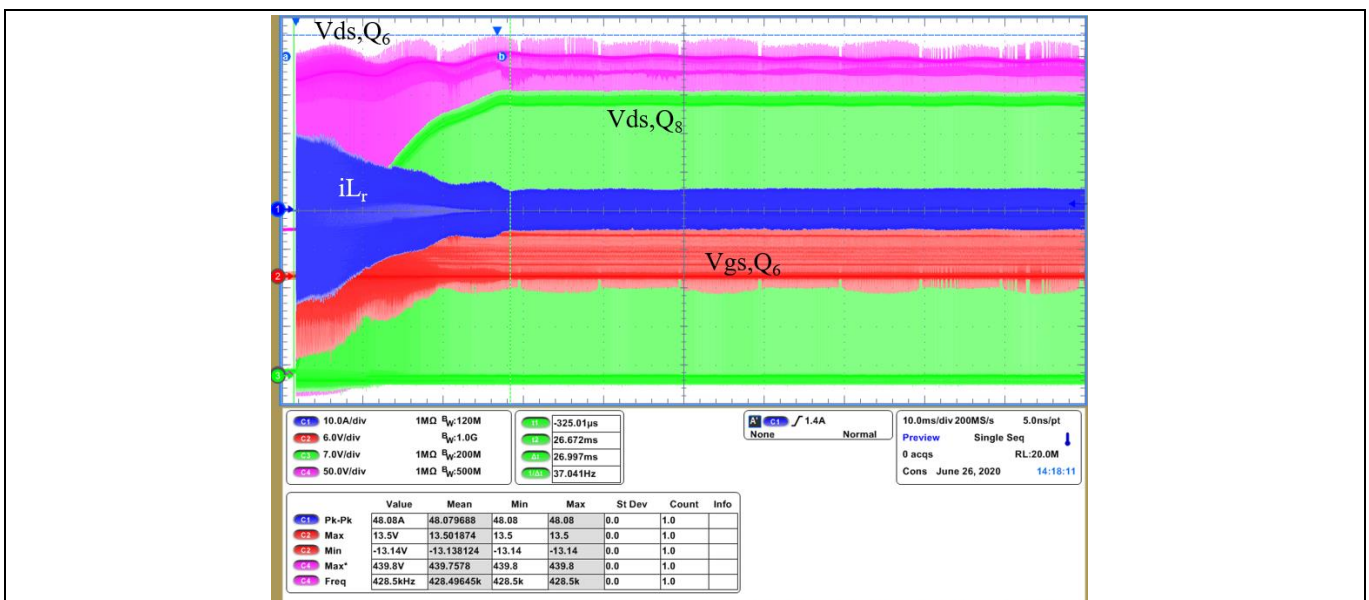


Figure 35 Soft-start sequence of the LLC converter at 10 A load while integrated into the complete PSU

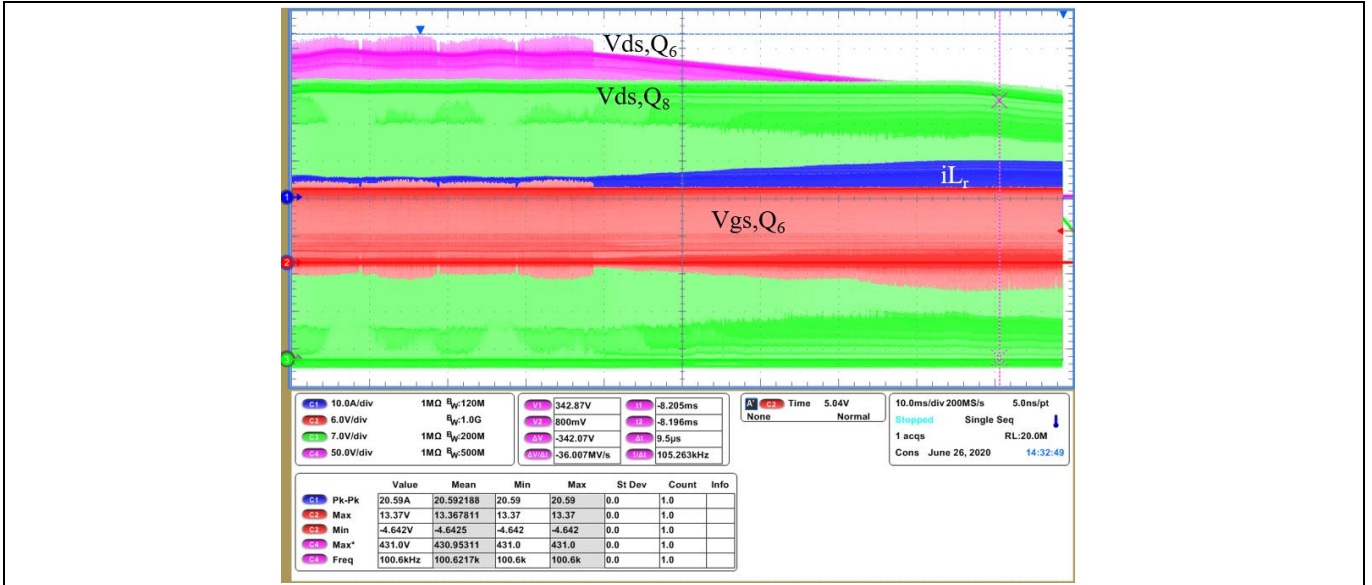


Figure 36 Brown-out sequence of the LLC converter at 10 A load while integrated into the complete PSU

3.3.1 Hold-up time

The OCP V3 specifications require up to 20 ms hold-up time at full power, although the output voltage of the PSU is allowed to drop down to $48 V_{DC}$. It is worth mentioning that the Rack & Power specifications include a battery unit at the rack level, which continues to provide power to the system at $48 V_{DC}$ if the V_{AC} , and therefore the PSU output voltage, is missing.

Figure 37 shows a capture of the response totem pole PFC and the output voltage of the PSU during a 20 ms hold-up time at full power. Meanwhile **Figure 38** shows a capture of the response of the totem pole and the PSU during a 20 ms hold-up time at full power repeatedly.

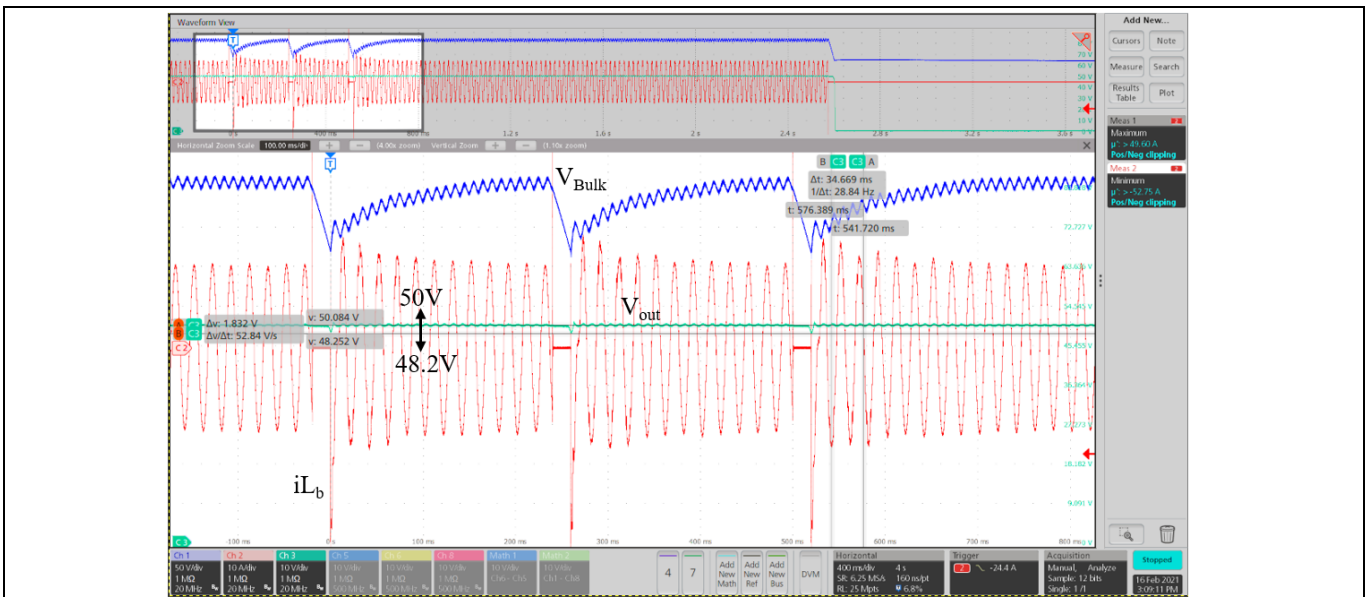


Figure 37 Detail view of 20 ms hold-up time at 60 A load and 230 V_{AC}

Experimental results

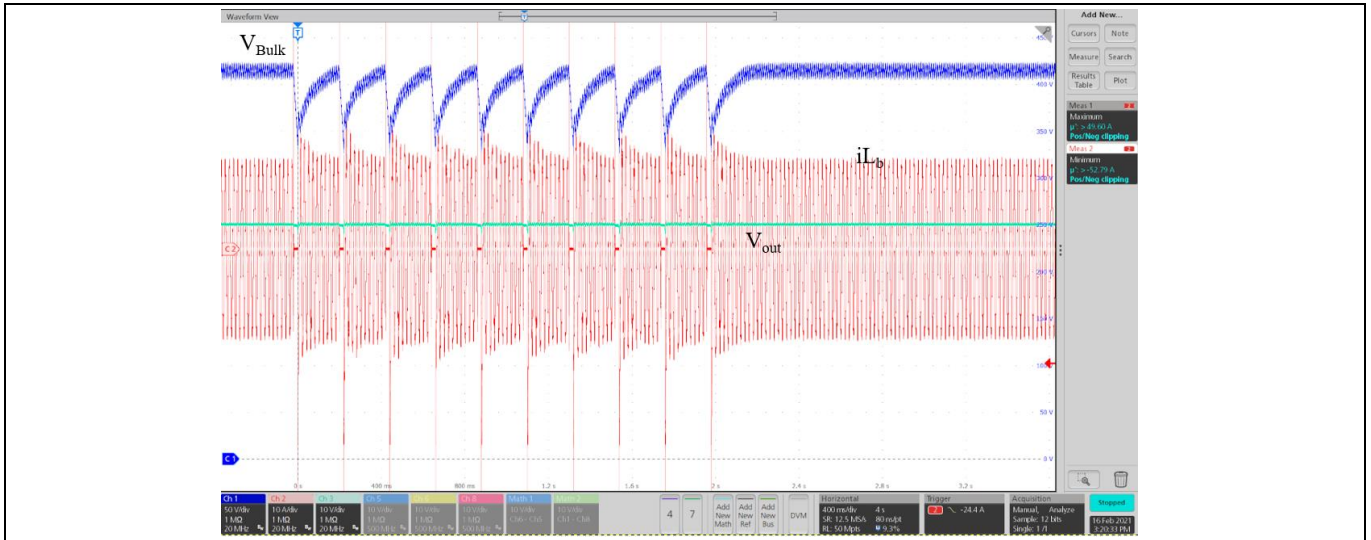


Figure 38 20 ms hold-up time at 60 A load and 230 V_{AC}. Ten times sequence at 200 ms intervals.

3.3.2 Temperature

The temperature of the converter has been measured outside and inside of its chassis. The temperature image in [Figure 39](#), captured with the PSU outside of its chassis, enables identification of the main hot-spots within the converter, which happen also to be the main sources of losses, discussed earlier in this document. More specifically, we can identify in the lower-left corner the main transformer and the secondary-side SRs, and in the upper-right corner the boosting half-bridge of the totem pole PFC.

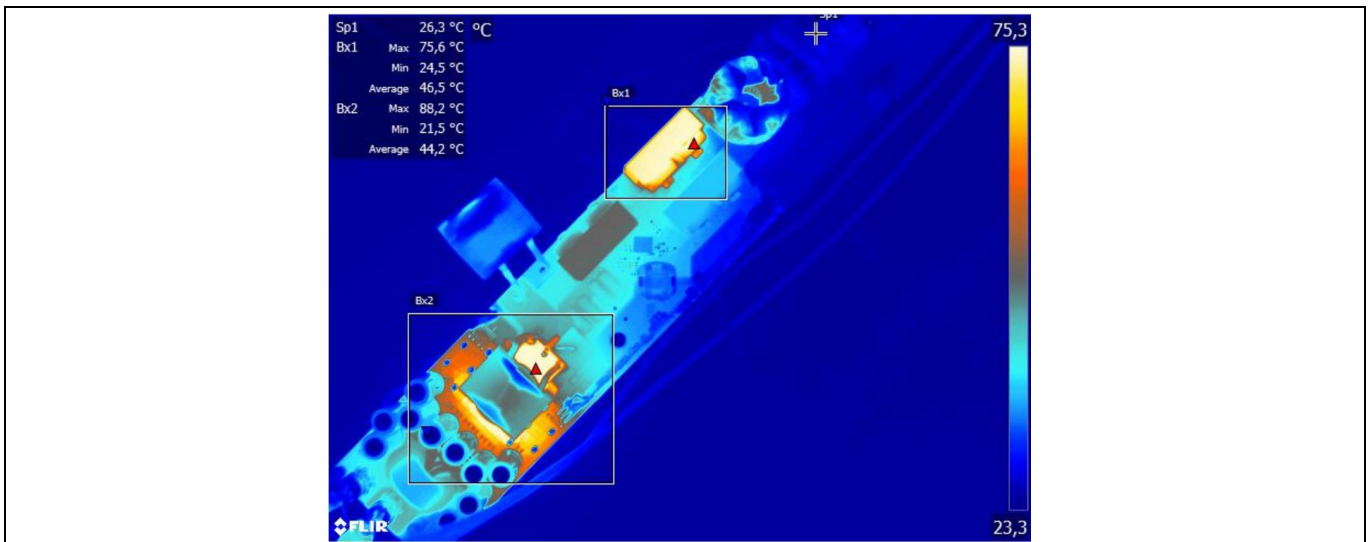


Figure 39 Measured temperature of the complete power supply prototype at full load, 230 V_{AC} and outside of its chassis

The temperature of the identified hot-spots was also measured at the minimum input voltage (180 V_{AC}) and with the PSU enclosed in the chassis and the internal fan supplied by the internal auxiliary bias. The measured temperatures, registered after running the converter for 30 minutes at full load, have been plotted in [Figure 40](#).

Experimental results

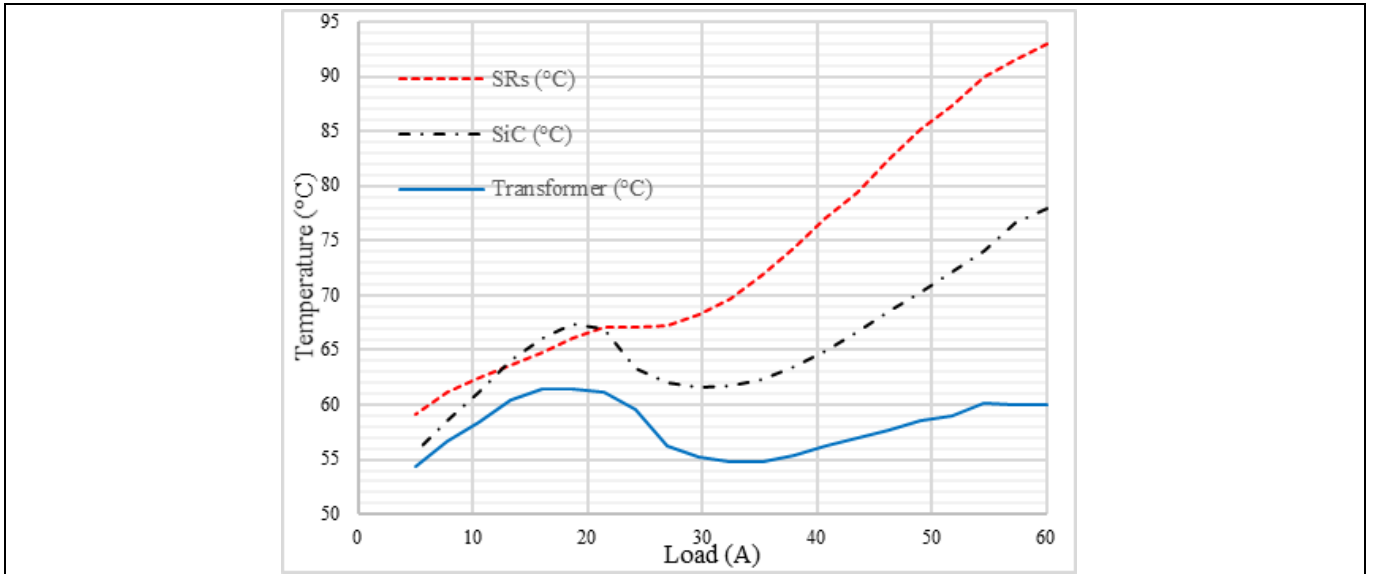


Figure 40 Measured temperature of the complete power supply prototype at full load, 180 V_{AC} and inside of its chassis

3.3.3 Efficiency

The efficiency of the complete power supply has been measured after running the converter for 30 minutes at full load. While the peak efficiency of the PSU not including the internal fan reaches 97.5 percent, it falls down to 97.47 percent when the consumption of the internal fan is also included (as required by OCP V3). Therefore, the overall efficiency of the PSU is slightly under the target specifications at the 230 V input voltage.

On the other hand, at full load the efficiency is also slightly under the requirements (Figure 41). However, at lighter loads the measurements exceed the limits by some margin.

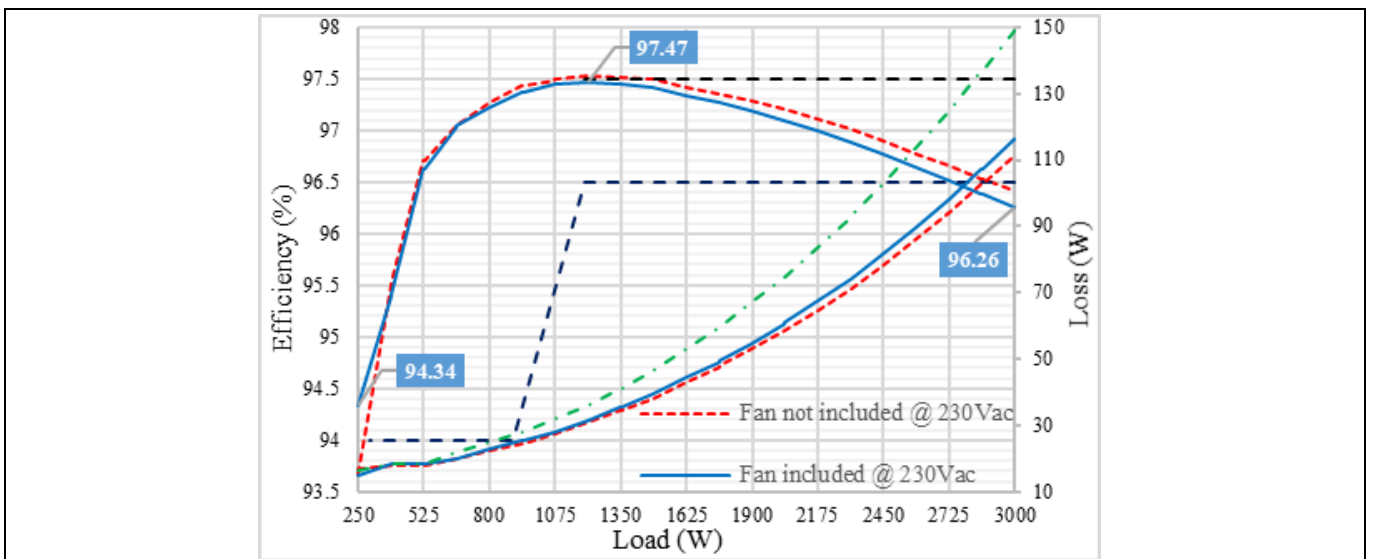


Figure 41 Measured efficiency of the complete power supply prototype at 230 V_{AC}

3.3.4 Power factor and THD

The power factor and THD have been measured at several input voltages within the input voltage range specifications. In accordance with these measurements the PSU complies with both the PF (Figure 42) and the THD (Figure 43) requirements of the OCP V3 specifications.

Experimental results

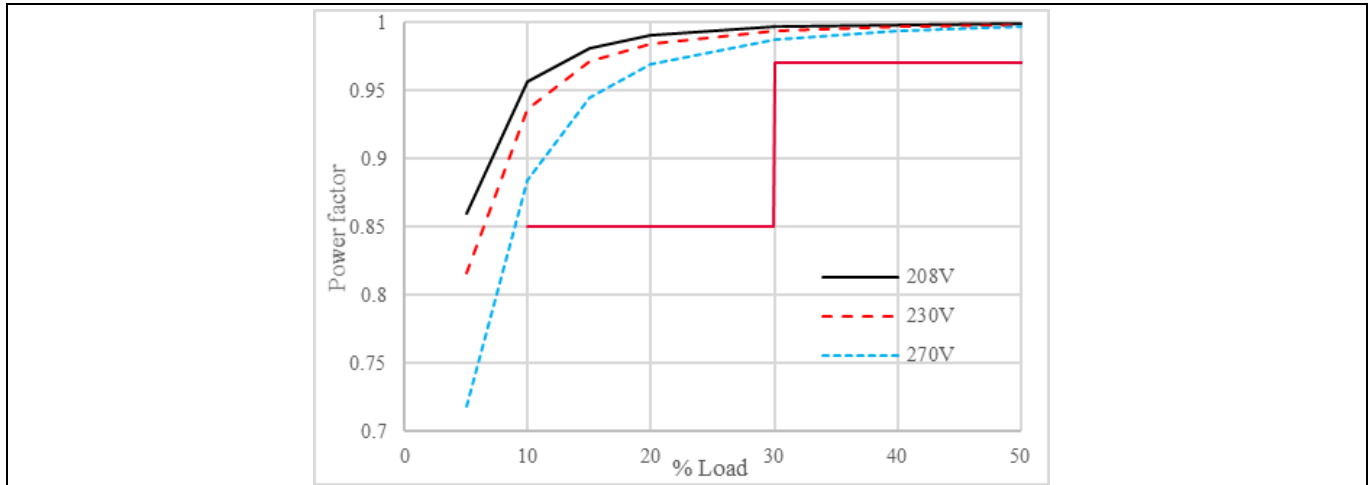


Figure 42 Measured PF of the complete power supply prototype at several input voltages. The specification limits are shown in red.

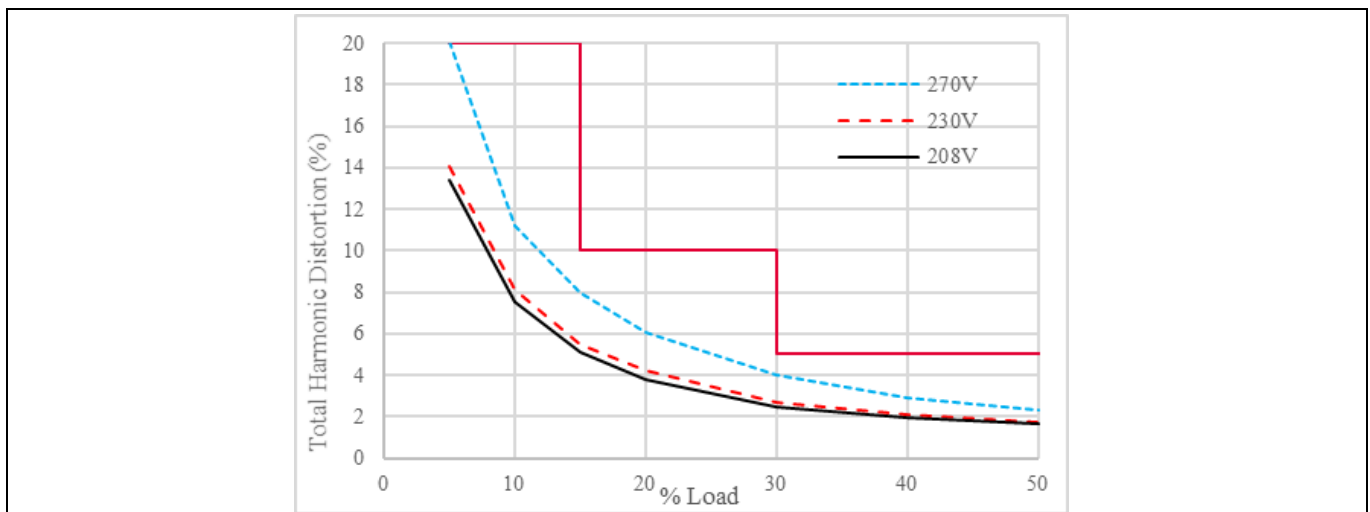


Figure 43 Measured THD of the complete power supply at several input voltages. The specification limits are shown in red.

3.3.5 EMI

Finally, the conducted electromagnetic interference (EMI) of the converter has been measured operating at 2.5 kW of load with a passive resistive load. **Figure 42** and **Figure 43** show the results of the average, the peak and the quasi-peak measurements. While the peak measurement touches the quasi-peak limit at some frequencies (blue curve in **Figure 44**), when measuring the quasi-peak (blue waveform in **Figure 45**), a very wide margin of more than 10 dB can be observed. Moreover, a wide margin of more than 10 dB can also be observed for the average measurement (green curve in **Figure 44** and **Figure 45**).

Experimental results

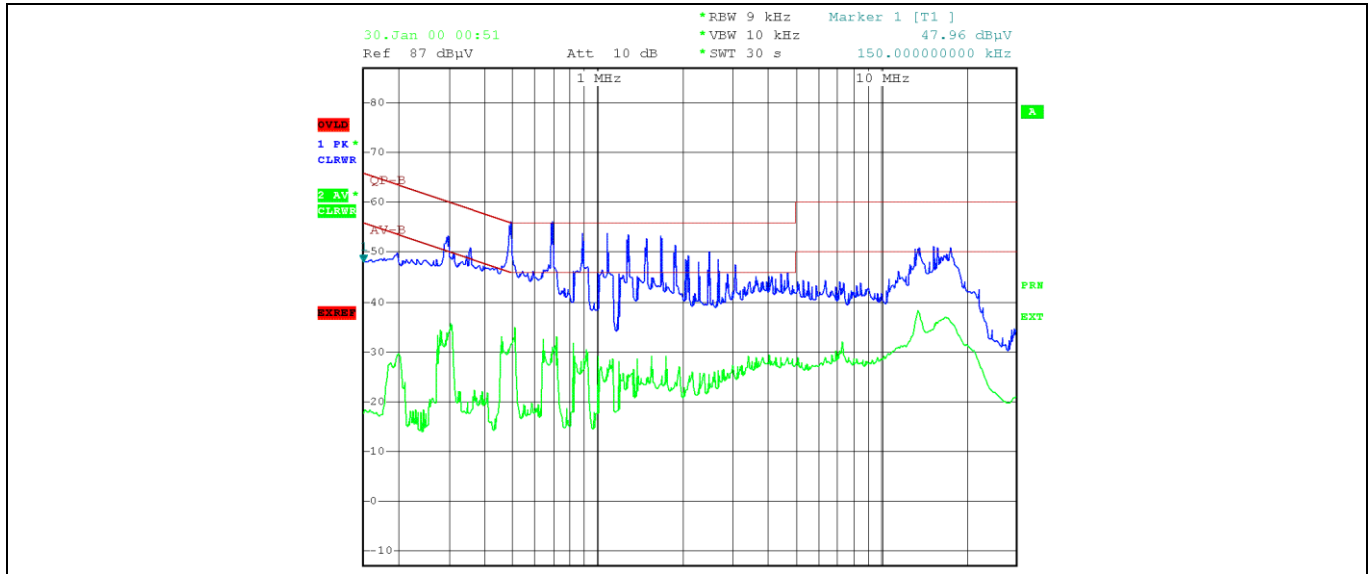


Figure 44 Measured EMI spectrum of the complete power supply prototype at 230 V_{AC} and 2.5 kW. Peak is shown in blue and average in green.

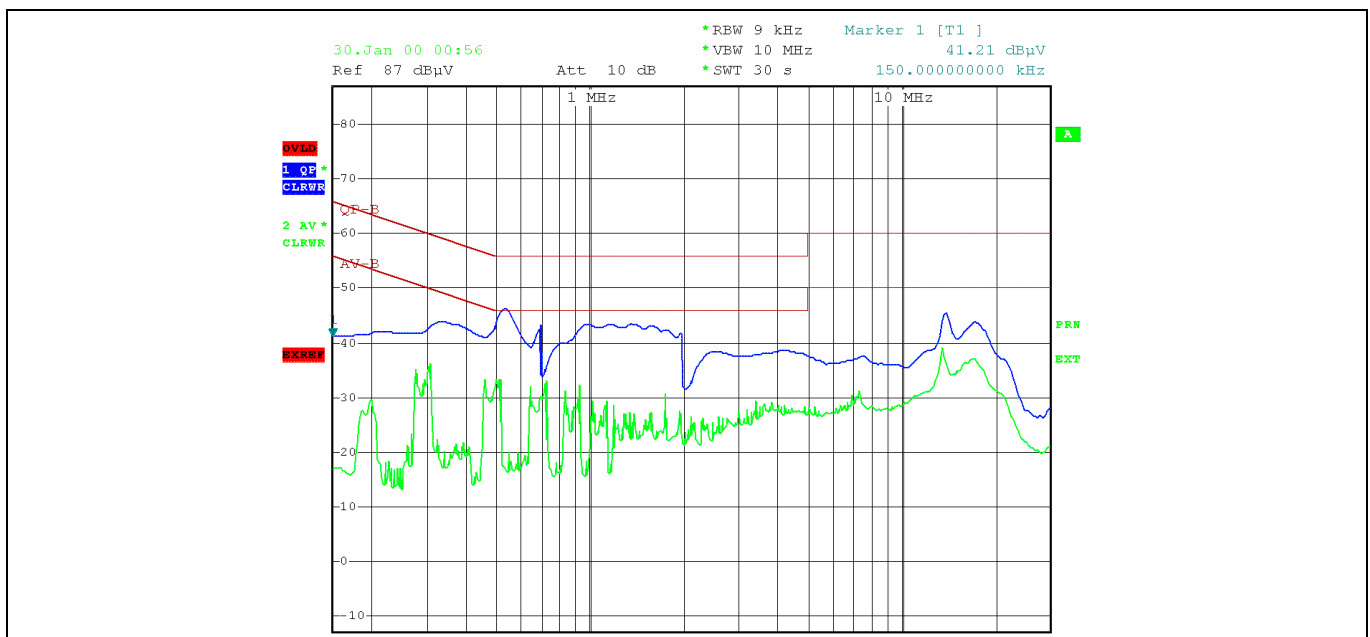


Figure 45 Measured EMI spectrum of the complete power supply prototype at 230 V_{AC} and 2.5 kW. Quasi-peak is shown in blue and average in green.

Design tips

4 Design tips

This section gives a summary of several features worth mentioning with regard to the hardware design of the PSU attaining the power semiconductors.

4.1 Driving 4-pin CoolSiC™

For the best performance of the boosting half-bridge of the totem pole AC-DC converter the use of devices in 4-pin packages with Kelvin source connection is recommended. The Kelvin source connection diminishes the negative feedback in the driving loop caused by the power source path, reducing the switching losses in hard-switched or hard-commutated topologies.

For the driving of the CoolSiC™ MOSFETs the recommended driver is the 1EDB9275F, which is a single-channel driver with a 14.4 V UVLO, specially designed for CoolSiC™ (Figure 46).

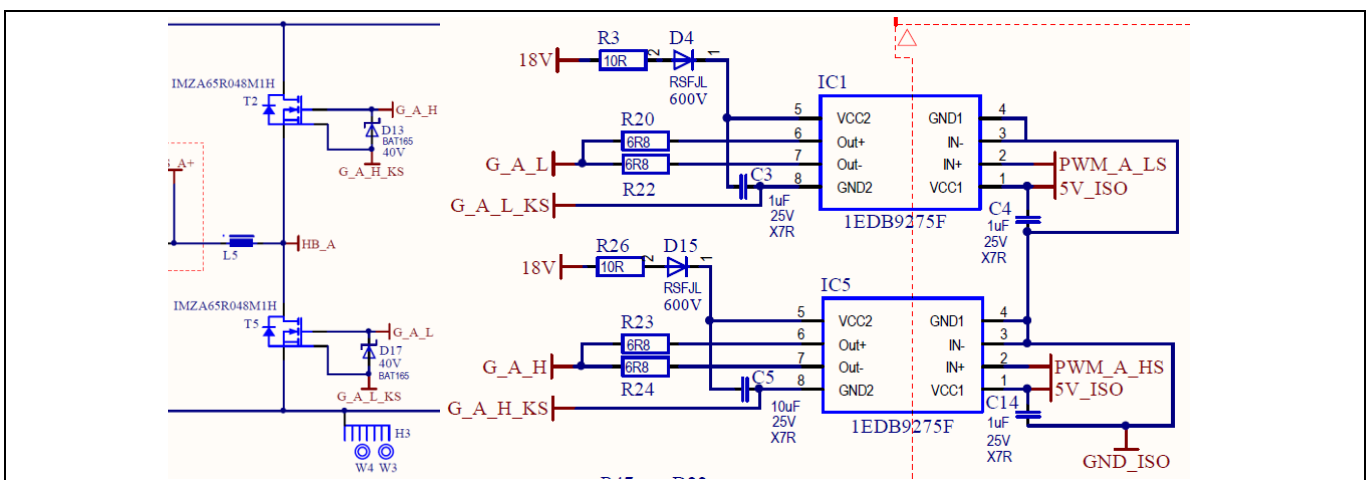


Figure 46 Recommended driving circuitry for the boosting half-bridge in the totem pole PFC

4.2 Driving 3-pin CoolMOS™

The SRs in the totem pole AC-DC converter are ZCS and at only twice the frequency of the grid (100 Hz to 120 Hz). Therefore, the switching speed is not critical. Moreover, a high-ohmic turn-on helps reduce common-mode noise caused by the transition of the SRs.

The recommended driving circuitry (Figure 47) includes two single-channel drivers (1EDB8275F), especially designed for driving CoolMOS™, with a UVLO of 7 V.

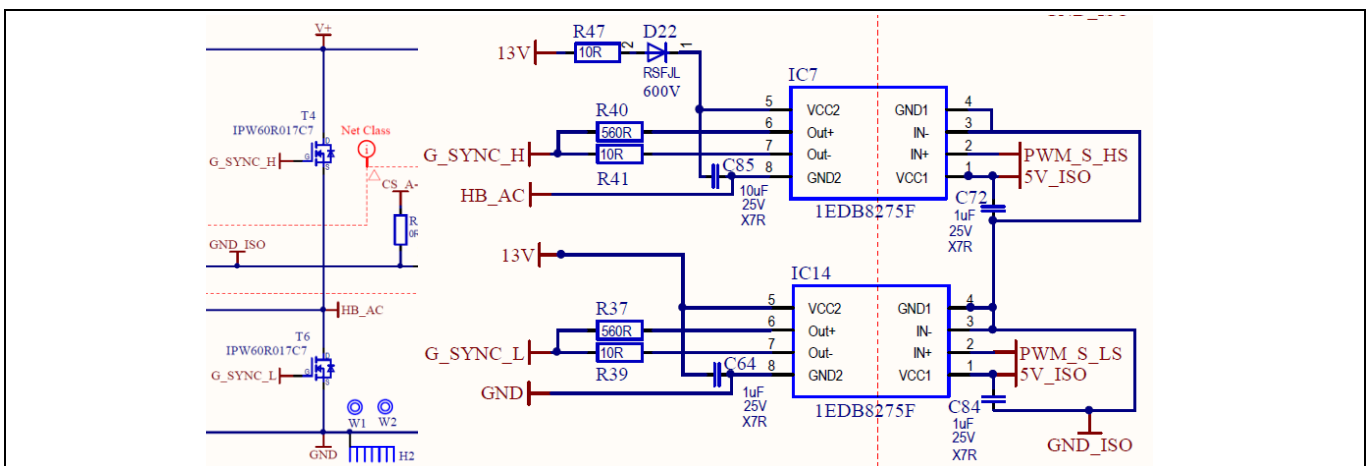


Figure 47 Recommended driving circuitry for the SRs in the totem pole PFC

Design tips

The primary-side devices in the half-bridge LLC are ZVS turn-on and hard-switched turn-off at relatively low currents (therefore lossless). Because of this, 4-pin devices with Kelvin source connection are not strictly needed. Therefore, in the PSU the primary-side MOSFETs are designed in 3-pin TO-247 packages.

The recommended driving circuitry (**Figure 48**) also includes two single-channel drivers, 1EDB8275F, designed for CoolMOS™. It is worth mentioning that the safety isolation in the LLC half-bridge driving is not required in this case because a digital isolator has been used to transfer the signal from the secondary side, where the LLC controller is located.

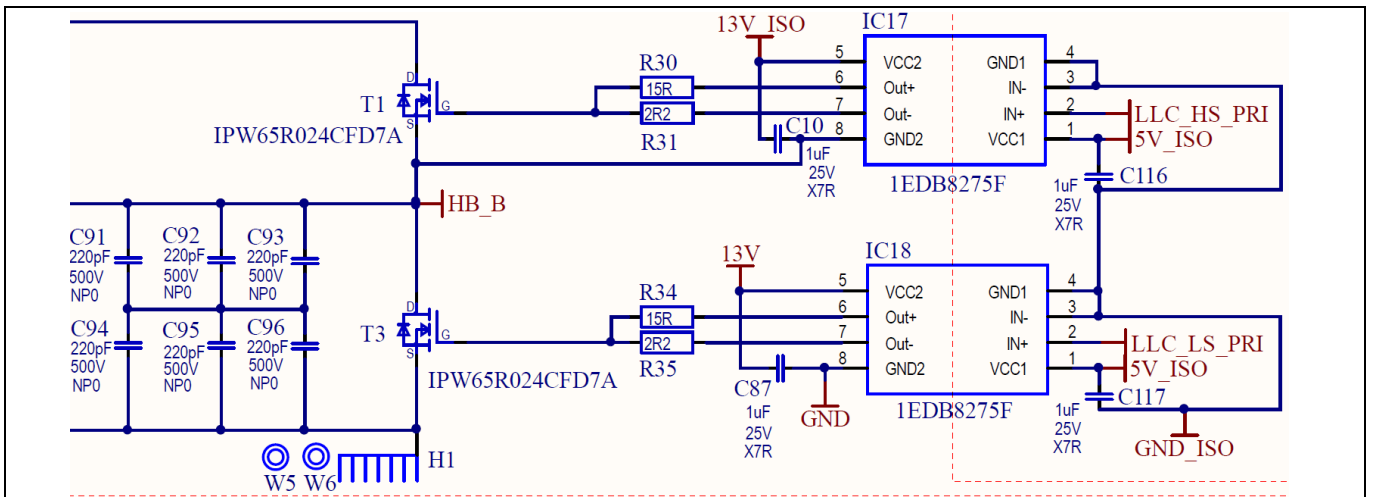


Figure 48 Recommended driving circuitry for the primary-side devices in the half-bridge LLC

4.3 Driving the ORing OptiMOS™

The ORing MOSFETs are located in the positive rail of the output of the PSU. Therefore, the driving of the ORing devices shall be referenced to the 50 V_{DC} output. To generate the required auxiliary voltage the proposed circuit in **Figure 49** is used.

The principle of operation of the circuit is of a capacitive charge pump. The capacitor C120 is referenced to one of the secondary-side SRs' half-bridge mid-point, which during the operation of the converter alternates between ground and the output voltage of the PSU at the switching frequency of the converter (square wave). Therefore, thanks to the decoupling diodes D9 and D5, the capacitor C120 is alternately charged from the auxiliary 12 V_{DC}, and discharged to the capacitor C119. Finally, the capacitor C119 supplies the ORing driver with 12 V_{DC} above the output PSU rail.

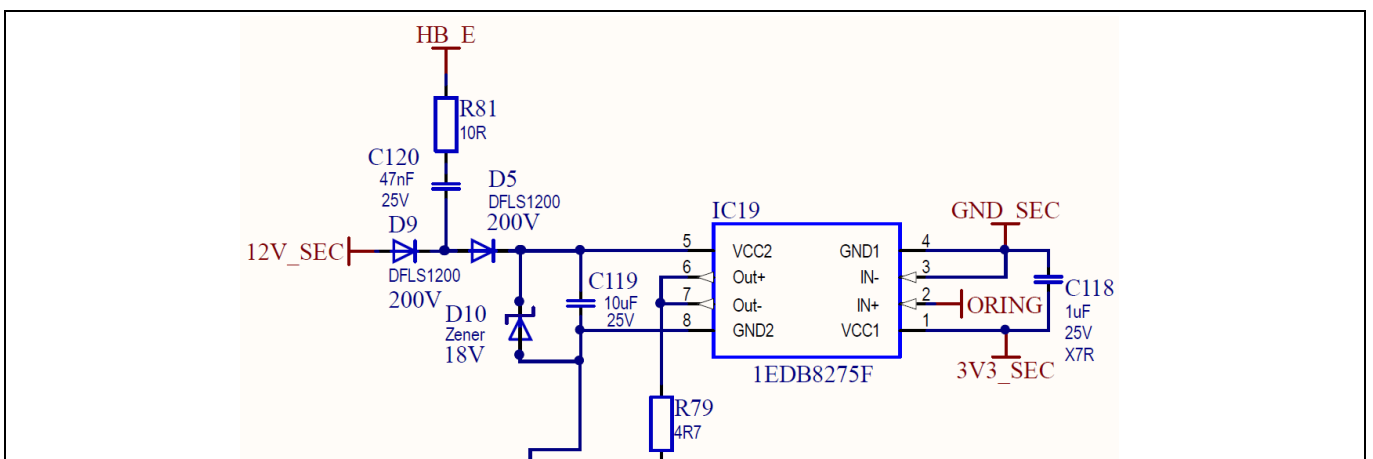


Figure 49 Proposed driving circuit for the ORing of the PSU

Design tips

4.4 Driving the SR OptiMOS™

The rectification of the half-bridge LLC DC-DC converters has a full-bridge configuration with a total of 24 devices, six devices per slot. Although the SRs are switched on and off in ZVS, and there are no switching losses caused by slow switching, it is still recommended to have four separate drivers. On one hand, the driving losses can be better spread between the four packages. On the other hand, the additional driver strength helps ensure accurate and fast switch-on and -off and proper clamping of the Miller feedback during the transitions.

The driving circuit for the SRs (Figure 50) includes four 2EDF7275F dual-channel, functional isolated MOSFET gate drivers, with up to 650 V_{DC} isolation channel-to-channel.

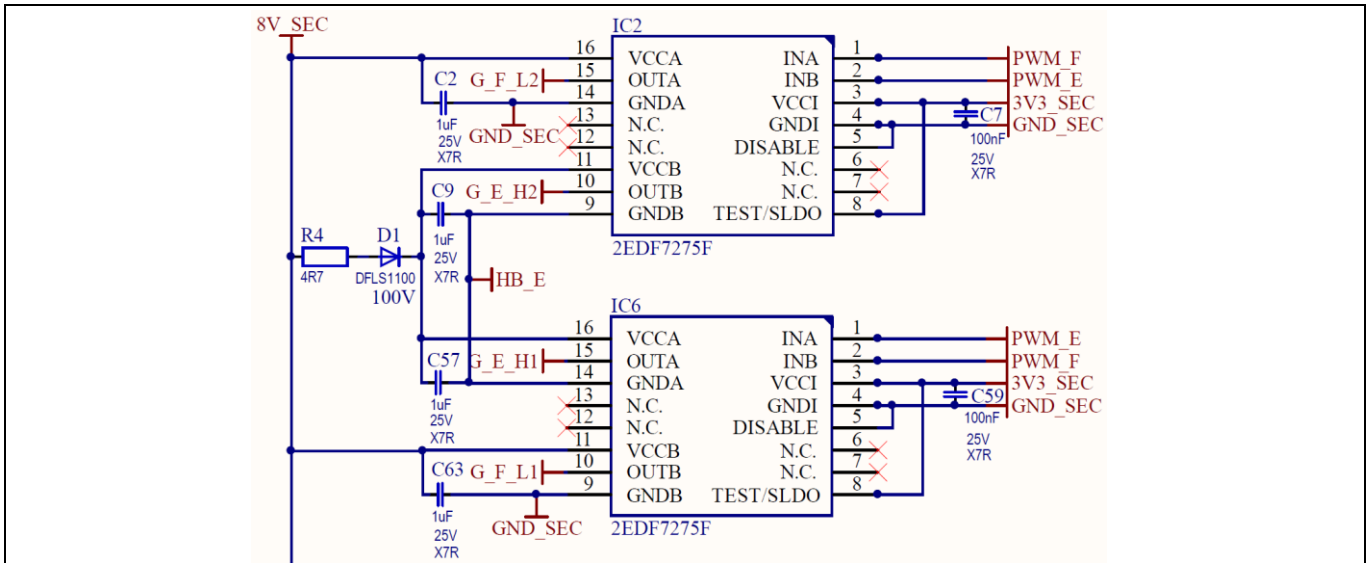


Figure 50 Proposed driving circuitry for the SRs of the LLC DC-DC converter

4.5 Generating the multiple auxiliary driving voltages

The complete PSU requires several distinct supply voltage rails:

- 3.3 V_{DC} for the supply of the LLC DC-DC control circuitry (XMC4200)
- 5 V_{DC} for the supply of the totem pole AC-DC control circuitry (XMC1404)
- 8.5 V_{DC} for the driving of the LLC DC-DC converter SRs (OptiMOS™)
- 12 V_{DC} for the driving of the primary-side half-bridge of the LLC DC-DC converter and the driving of the totem pole AC-DC converter SRs (CoolMOS™), and the supply of the internal fan
- 18 V_{DC} for the driving of the boosting half-bridge in the totem pole AC-DC converter (CoolSiC™)

The onboard auxiliary flyback provides several of these supply rails. However, it is not practical to realize a flyback transformer with that many distinct windings. Therefore, the auxiliary circuitry proposed in Figure 50 provides several of the above listed voltages from one of the flyback 12 V_{DC} outputs.

The core of the circuit in Figure 51 is a 1EDB8275F single-channel driver, which generates a fixed-frequency square wave at its output (approximately 350 kHz). The square wave is fed to two different smaller converters. On the one hand, a charge pump (C101 and D28) raises the 12 V_{DC} at the input up to 24 V_{DC} (at C99), which is then regulated down to 18 V_{DC} by an LDO (C98 and IC8). On the other hand, a three-winding transformer with voltage-doubler rectification generates two separate isolated supply rails for the totem pole PFC control card and the high-side driver of the half-bridge LLC.

Design tips

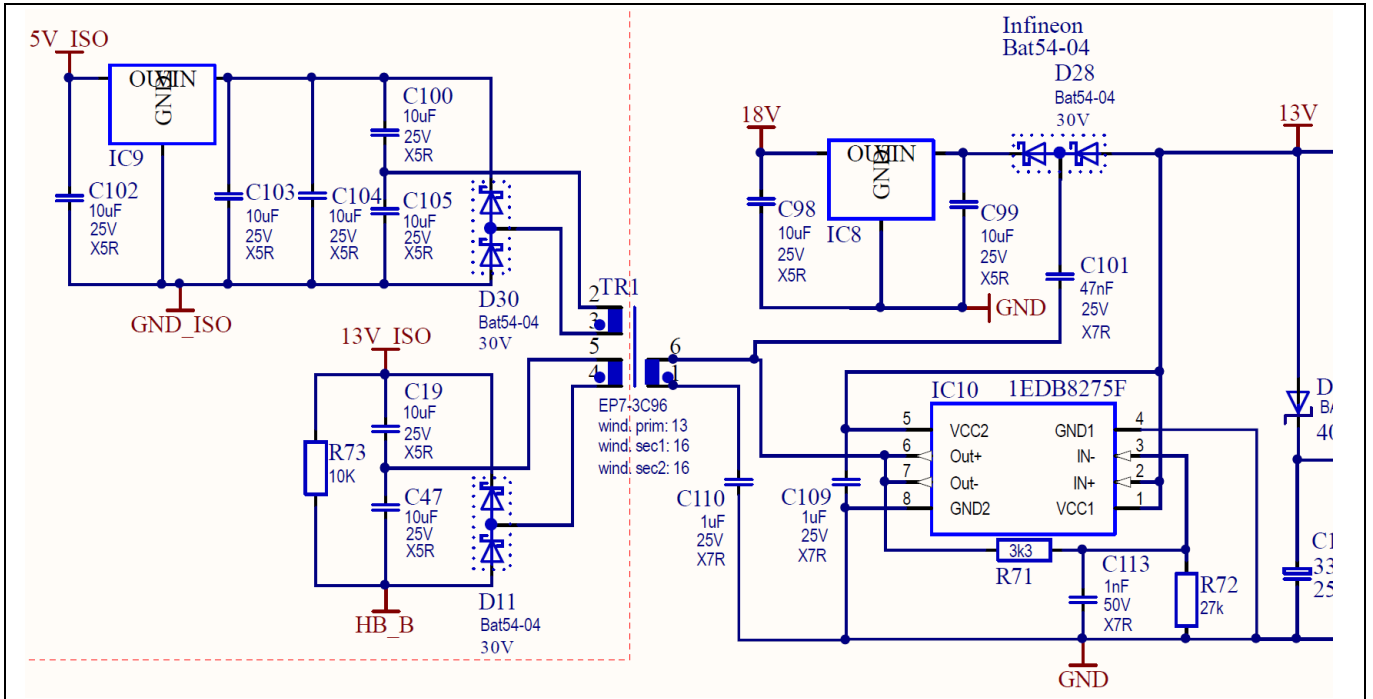
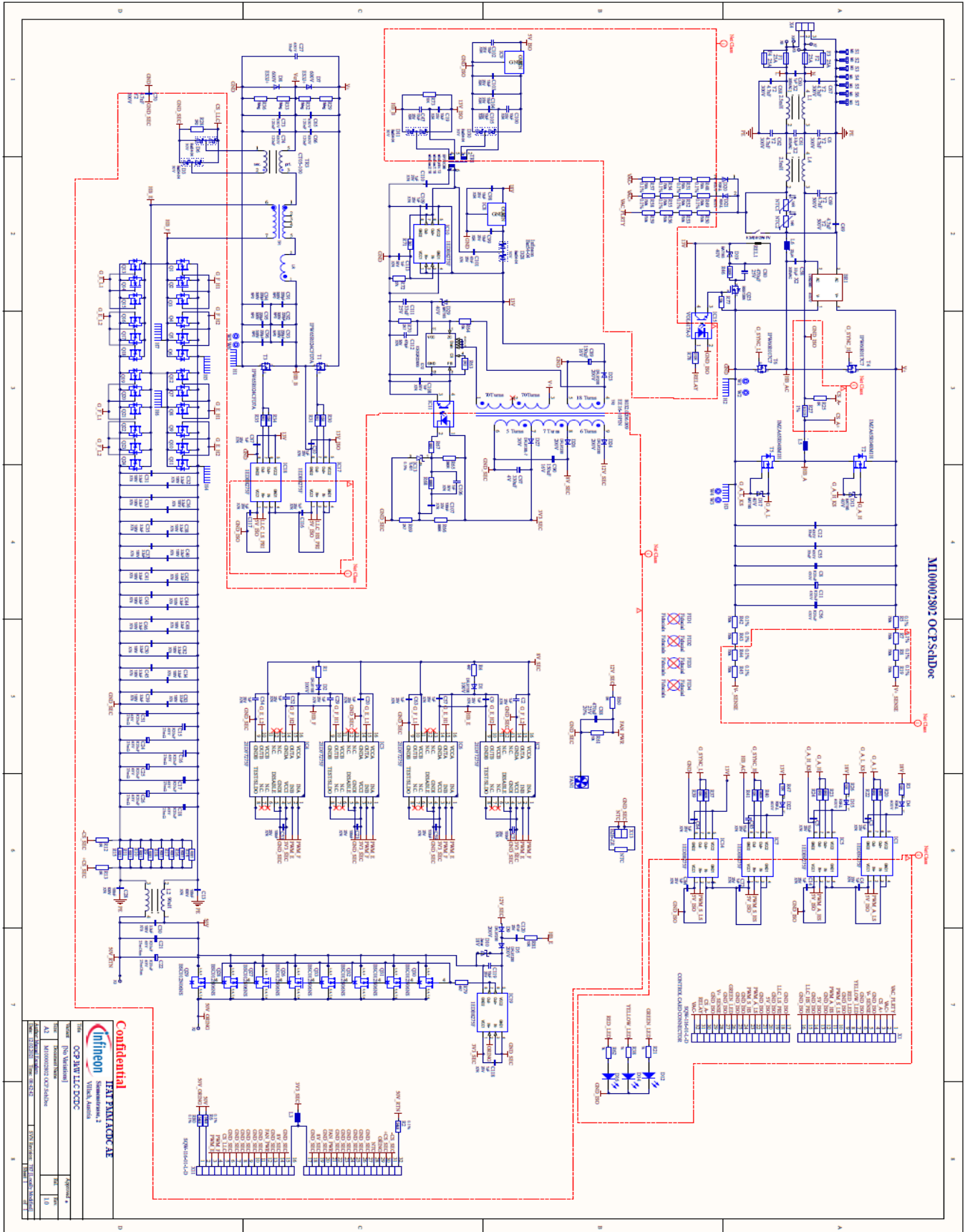


Figure 51 Proposed auxiliary supply circuit implemented with the single-channel driver 1EDB8275F

5 Schematics

5.1 Main board

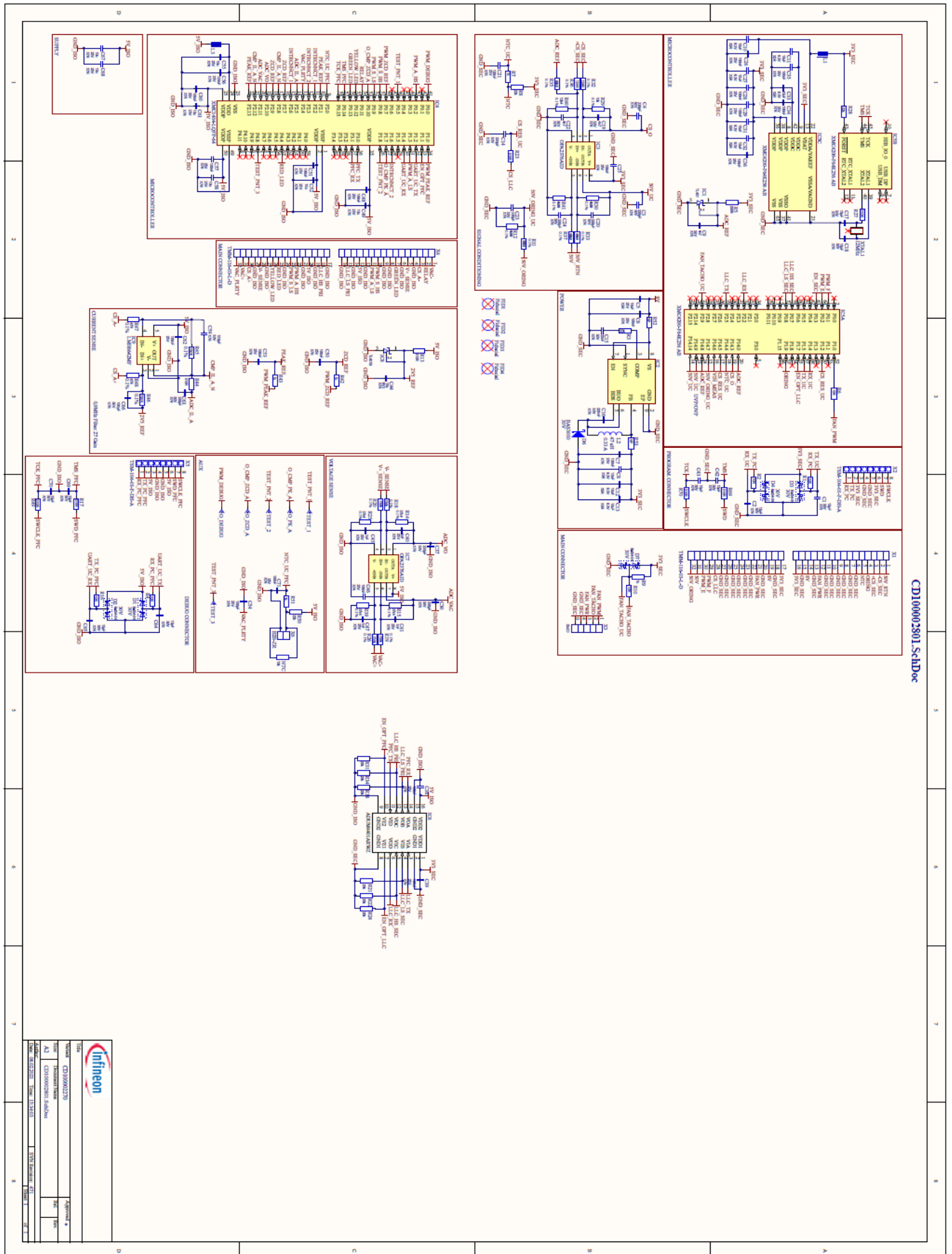


Server and data center 3 kW 50 V PSU

EVAl_3KW_50V_PSU

Schematics

5.2 Control card



Schematics

5.3 Bill of materials

The complete BOM is available from the downloads section of the Infineon website. A log-in is required to download this material.

Table 3 BOM of the main board

S. no.	Ref. designator	Description	Manufacturer	Part no.
2	T1, T3	MOSFET	Infineon	IPW65R035CFD7A
2	T2, T5	MOSFET	Infineon	IPZA65R062M1
2	T4, T6	MOSFET	Infineon	IPW60R017C7
1	Q25	MOSFET	Infineon	BSS138N
8	Q26, Q27, Q28, Q29, Q30, Q31, Q32, Q33	MOSFET	Infineon	BSC012N06NS
24	Q1, Q2, Q3, Q4, Q5, Q6, Q7, Q8, Q9, Q10, Q11, Q12, Q13, Q14, Q15, Q16, Q17, Q18, Q19, Q20, Q21, Q22, Q23, Q24	MOSFET	Infineon	BSC037N08NS5
1	IC12	Quasi-resonant controller	Infineon	ICE2QR2280G
2	IC1, IC5	Single-channel MOSFET gate driver IC	Infineon	1EDB9275F
4	IC2, IC3, IC4, IC6	MOSFET gate driver IC	Infineon	2EDF7275F
6	IC7, IC10, IC14, IC17, IC18, IC19	Single-channel MOSFET gate driver IC	Infineon	1EDB8275F
5	D3, D6, D11, D28, D30	Schottky diode	Infineon	BAT54-04
4	D13, D17, D19, D29	Schottky diode	Infineon	BAT165
1	BR1	Bridge diode	Vishay	LVB2560
9	C2, C9, C20, C29, C52, C54, C57, C63, C118	Ceramic capacitor		1 μ F
12	C3, C4, C10, C14, C64, C72, C84, C87, C109, C110, C116, C117	Ceramic capacitor		1 μ F
12	C5, C19, C47, C85, C98, C99, C100, C102, C103, C104, C105, C119	Ceramic capacitor		10 μ F
4	C6, C49, C62, C69	Ceramic capacitor	Vishay	4.7 nF
4	C7, C23, C53, C59	Ceramic capacitor		100 nF
3	C8, C11, C56	Electrolytic capacitor	Rubycon	820 μ F
3	C12, C27, C55	Foil capacitor	EPCOS-TDK	33 nF
2	C13, C28	Ceramic capacitor	KEMET	100 nF
9	C15, C16, C18, C21, C22, C24, C25, C26, C51	Electrolytic capacitor	Rubycon	820 μ F
21	C30, C31, C32, C33, C34, C35, C36, C37, C38, C39,	Ceramic capacitor	TDK	3.3 μ F

Schematics

S. no.	Ref. designator	Description	Manufacturer	Part no.
	C40, C41, C42, C43, C44, C45, C46, C48, C50, C82, C83			
2	C58, C61	Foil capacitor	Würth	3.3 μ F
1	C60	Foil capacitor	TDK	1 μ F
4	C65, C66, C73, C74	Foil capacitor	Panasonic	120 nF
2	C80, C88	Electrolytic capacitor	Panasonic	470 μ F
2	C89, C90	Polarized capacitor	Panasonic	150 μ F
6	C91, C92, C93, C94, C95, C96	Ceramic capacitor	AVX	220pF
1	C97	Polarized capacitor	KEMET	330 μ F
1	C101	Ceramic capacitor		47 nF
3	C106, C108, C113	Ceramic capacitor		1 nF
1	C107	Ceramic capacitor		100 nF
1	C111	Polarized capacitor	Vishay	33 μ F
1	C112	Ceramic capacitor		470 pF
1	C120	Ceramic capacitor		47 nF
2	D1, D2	Standard diode	Diodes Inc.	DFLS1100
5	D4, D15, D20, D21, D22	Diode	Taiwan Semiconductor	RSFJL
5	D5, D9, D23, D24, D26	Diode	Diodes Inc.	DFLS1200
2	D7, D8	Standard diode	ON Semiconductor	ES3J+
1	D10	Schottky diode	ON Semiconductor	MMSZ5248BT1G
1	D12	LED	Osram	LG T67K-H2K1-24
1	D14	LED	Osram	LY T676-S1T1-26
1	D16	LED	Osram	LS T670-J1K2-1
1	D27	Diode	Diodes Inc.	DFLS130L-7
4	F1, F2, F3, F4	Fuse	Littelfuse	01220083Z
3	H1, H2, H3	Heatsink	Fisher	SK 448 40 2 x M3L
2	H4, H5	Heatsink	HTSK GmbH	HT10000280
1	IC8	Integrated circuit	ST Microelectronics	L78L18ACUTR
1	IC9	Integrated circuit	ST Microelectronics	L78L05ACUTR
2	IC11, IC15	Integrated circuit	Vishay	VOL617A-3
1	IC13	Integrated circuit	Texas Instruments	TL431BCDBZR
2	L1, L4	Inductor	ICE	MG10000841
1	L2	Inductor	ICE	MG100002271
1	L3	Inductor	Würth	742792602
1	L5	Inductor	ICE	MG300002800
1	LR	Inductor	ICE	MG300002803
1	NTC	Resistor	Vishay	NTCALUG03A103GC

Schematics

S. no.	Ref. designator	Description	Manufacturer	Part no.
2	NTC1, NTC2	NTC resistor	Ametherm	995-SL22-14007
3	R1, R4, R79	Resistor		4R7
3	R2, R6, R80	Resistor	Yageo	RC0603FR-0754K9L
4	R3, R26, R47, R81	Resistor		10 R
20	R5, R7, R8, R19, R42, R43, R44, R45, R48, R49, R50, R51, R52, R53, R54, R55, R56, R57, R58, R59	Resistor		750 k
8	R9, R10, R11, R14, R15, R16, R17, R18	Resistor	TT Electronics	LRMAT2512-R001FT4
2	R12, R13	Resistor		0 R
4	R20, R22, R23, R24	Resistor		6R8
3	R21, R38, R62	Resistor		1 k
1	R25	Resistor		0 R
1	R27	Resistor	TT Electronics	LRMAT2512-R003FT4
2	R28, R63	Resistor		2R2
4	R29, R32, R33, R36	Resistor		1 Meg
2	R30, R34	Resistor		15 R
2	R31, R35	Resistor		2R2
2	R37, R40	Resistor		560 R
2	R39, R41	Resistor		10 R
1	R46	Resistor		330 R
1	R60	Resistor		0 R
1	R61	Resistor		10 k
2	R64, R77	Resistor		15 k
1	R65	Resistor		390 R
2	R66, R68	Resistor		866 R
1	R67	Resistor		68 R
2	R69, R70	Resistor		2K7
1	R71	Resistor		3k3
1	R72	Resistor		27 k
1	R73	Resistor		10 k
1	R78	Resistor		510 R
1	REL1	Relay	Fujitsu	FTR-K3AB012W-PV
1	TF1	Transformer	ICE	MG300002804
1	TF2	Transformer	ICE	ICE200221
1	TR1	Transformer	ICE	8034.0103.015
1	TR3	Current transformer	ICE	CT05-100
6	W1, W2, W3, W4, W5, W6	Nylon washer	Keystone Electronics	3195

Schematics

S. no.	Ref. designator	Description	Manufacturer	Part no.
2	X1, X11	Header 2x16 contacts	Samtec	SQW-116-01-L-D
2	X2, X3	Connector	Ettinger.de	13.40.596
1	X4	Connector	Phoenix Contact	1714968
4	X5, X6, X7, X8	Connector	TE Connectivity	1217169-1
1	X13	Connector	JST	B2B-ZR

Table 4 BOM of the control card

S. no.	Ref. designator	Description	Manufacturer	Part no.
1	IC4	32-bit microcontroller	Infineon	XMC1404-LQFP-64
1	IC5	32-bit microcontroller	Infineon	XMC4200-F64K256 AB
5	D1, D2, D3, D4, D7	Schottky diode	Infineon	BAT54-04
1	D6	Schottky diode	Infineon	BAS3010
1	IC2	IC buck	Infineon	IFX91041EJ V33
10	C1, C2, C17, C18, C42, C43, C64, C65, C69, C70	Ceramic capacitor		15 pF
9	C3, C4, C14, C20, C23, C24, C30, C37, C63	Ceramic capacitor		330 pF
1	C5	Ceramic capacitor		10 µF
22	C6, C7, C21, C25, C26, C28, C29, C34, C35, C36, C38, C39, C46, C48, C50, C51, C53, C56, C57, C60, C62, C71	Ceramic capacitor		100 nF
9	C8, C10, C11, C12, C13, C27, C31, C32, C33	Ceramic capacitor		10 µF
3	C9, C19, C22	Ceramic capacitor		4 n7
1	C15	Ceramic capacitor		22 nF
1	C16	Ceramic capacitor		220 nF
4	C40, C41, C45, C47	Ceramic capacitor		1 nF
1	C44	Ceramic capacitor		10 µF
7	C49, C52, C55, C58, C61, C67, C68	Ceramic capacitor		10 µF
3	C54, C59, C66	Ceramic capacitor		100 pF
1	IC1, IC8	Voltage reference	Texas Instruments	TL431BCDBZR
2	IC3, IC7	Op-amp	Texas Instruments	OPA2376AID
1	IC6	Digital isolator	Analog Devices	ADUM4401ARWZ
1	IC9	Op-amp	Texas Instruments	LMH6642MF
2	L1, L3	Ferrite bead	Würth	742792602
1	L2	SMD power inductor	Würth	74404042470

Schematics

S. no.	Ref. designator	Description	Manufacturer	Part no.
1	NTC	Resistor	Vishay	NTCALUG03A103GC
6	R1, R2, R4, R6, R10, R16	Resistor		10 R
4	R3, R8, R28, R50	Resistor		22 k
1	R5	Resistor		200 R
5	R7, R9, R42, R43, R51	Resistor		1 k
4	R11, R33, R35, R37	Resistor	TE Connectivity	CPF0603B49K9E1
3	R12, R30, R41	Resistor	Yageo	RT0603BRD074K99L
8	R13, R17, R23, R27, R44, R49, R69, R70	Resistor		510 R
4	R14, R15, R25, R39	Resistor	TE Connectivity	5-2176089-1
4	R18, R19, R20, R26	Resistor	Yageo	RT0805BRD07750KL
6	R21, R22, R24, R31, R34, R38	Resistor		20 k
1	R29	Resistor	Yageo	RT0603BRD0710KL
2	R32, R36	Resistor	TE Connectivity	CPF0603B124RE1
1	R40	Resistor	TT Electronics	PCF0603R-12K4BT1
2	R45, R46	Resistor	Panasonic	ERA3AEB751V
2	R47, R48	Resistor	Yageo	RT0603BRD0747RL
2	X1, X4	Connector	Samtec	TMM-116-03-L-D
2	X2, X5	Header 8 contacts	Samtec	TSM-104-01-F-DH-A
1	X3	Pin-header 5-pole	Molex	53398-0471
1	X6	Connector	JST	B2B-ZR
1	XTAL1	Crystal oscillator	Kyocera	CX3225GA12000D0PT VCC

6 References and appendices

6.1 Abbreviations and definitions

Table 5 Abbreviations

Abbreviation	Meaning
CE	Conformité Européenne
EMI	Electromagnetic interference
UL	Underwriters Laboratories

6.2 References

- [1] Open Compute Project, viewed 9 May 2021, <https://www.opencompute.org/>
- [2] Open Rack/SpecsAndDesigns, viewed 9 May 2021, https://www.opencompute.org/wiki/Open_Rack/SpecsAndDesigns
- [3] M. Kutschak, D. Meneses Herrera, “3300 W CCM bidirectional totem pole with 650 V CoolSiC™ and XMC™”, AN_1911_PL52_1912_141352, Infineon Technologies, January 2020
- [4] M. Kutschak, M. Escudero, “3300 W 52 V LLC with 600 V CoolMOS™ CFD7 and XMC™”, AN_1906_PL52_1906_094110, Infineon Technologies, January 2020
- [5] R. Siemieniec, R. Mente, W. Jantscher, D. Kammerlander, U. Wenzel and T. Aichinger, “650 V SiC Trench MOSFET for high-efficiency power supplies”, 2019 21st European Conference on Power Electronics and Applications (EPE '19 ECCE Europe), Genova, Italy, 2019, pp. 1–16
- [6] M. Escudero, M. Kutschak, N. Fontana, N. Rodriguez and D. P. Morales, “Non-Linear Capacitance of Si SJ MOSFETs in Resonant Zero Voltage Switching Applications”, in *IEEE Access*, vol. 8, 2020, pp. 116117–116131

Revision history

Revision history

Document version	Date of release	Description of changes
V 1.0	27-02-2021	First release

Trademarks

All referenced product or service names and trademarks are the property of their respective owners.

Edition 2021-02-27

Published by

Infineon Technologies AG

81726 Munich, Germany

© 2021 Infineon Technologies AG.

All Rights Reserved.

Do you have a question about this document?

Email: erratum@infineon.com

Document reference

ER_2102_PL52_2102_154546

For further information on the product, technology, delivery terms and conditions and prices please contact your nearest Infineon Technologies office (www.infineon.com).

WARNINGS

Due to technical requirements products may contain dangerous substances. For information on the types in question please contact your nearest Infineon Technologies office.

Except as otherwise explicitly approved by Infineon Technologies in a written document signed by authorized representatives of Infineon Technologies, Infineon Technologies' products may not be used in any applications where a failure of the product or any consequences of the use thereof can reasonably be expected to result in personal injury.

X-ON Electronics

Largest Supplier of Electrical and Electronic Components

Click to view similar products for [Power Management IC Development Tools](#) category:

Click to view products by [Infineon](#) manufacturer:

Other Similar products are found below :

[EVB-EP5348UI](#) [MIC23451-AAAYFL EV](#) [MIC5281YMME EV](#) [124352-HMC860LP3E](#) [DA9063-EVAL](#) [ADP122-3.3-EVALZ](#) [ADP130-0.8-EVALZ](#) [ADP130-1.8-EVALZ](#) [ADP1740-1.5-EVALZ](#) [ADP1870-0.3-EVALZ](#) [ADP1874-0.3-EVALZ](#) [ADP199CB-EVALZ](#) [ADP2102-1.25-EVALZ](#) [ADP2102-1.875EVALZ](#) [ADP2102-1.8-EVALZ](#) [ADP2102-2-EVALZ](#) [ADP2102-3-EVALZ](#) [ADP2102-4-EVALZ](#) [AS3606-DB](#) [BQ25010EVM](#) [BQ3055EVM](#) [ISLUSBI2CKIT1Z](#) [LM2734YEVAL](#) [LP38512TS-1.8EV](#) [EVAL-ADM1186-1MBZ](#) [EVAL-ADM1186-2MBZ](#) [ADP122UJZ-REDYKIT](#) [ADP166Z-REDYKIT](#) [ADP170-1.8-EVALZ](#) [ADP171-EVALZ](#) [ADP1853-EVALZ](#) [ADP1873-0.3-EVALZ](#) [ADP198CP-EVALZ](#) [ADP2102-1.0-EVALZ](#) [ADP2102-1-EVALZ](#) [ADP2107-1.8-EVALZ](#) [ADP5020CP-EVALZ](#) [CC-ACC-DBMX-51](#) [ATPL230A-EK](#) [MIC23250-S4YMT EV](#) [MIC26603YJL EV](#) [MIC33050-SYHL EV](#) [TPS60100EVM-131](#) [TPS65010EVM-230](#) [TPS71933-28EVM-213](#) [TPS72728YFFEVM-407](#) [TPS79318YEQEV](#) [UCC28810EVM-002](#) [XILINXPWR-083](#) [LMR22007YMINI-EVM](#)